MASTER COPY: PLEASE KEEP THIS "MEMORANDUM OF TRANSMITTAL" BLANK FOR REPRODUCTION PURPOSES. WHEN REPORTS ARE GENERATED UNDER THE ARO SPONSORSHIP, FORWARD A COMPLETED COPY OF THIS FORM WITH EACH REPORT SHIPMENT TO THE ARO. THIS WILL ASSURE PROPER IDENTIFICATION. NOT TO BE USED FOR INTERIM PROGRESS REPORTS; SEE PAGE 2 FOR INTERIM PROGRESS REPORT INSTRUCTIONS.

MEMORANDUM OF TRANSMITTAL

U.S. Army Research Office
ATTN: AMSRL-RO-BI (TR)
P.O. Box 12211
Research Triangle Park, NC 27709-2211

☐ Reprint (Orig + 2 copies)

☐ Technical Report (Orig + 2 copies)

☐ Manuscript (1 copy)

☒ Final Progress Report (Orig + 2 copies)

☐ Related Materials, Abstracts, Theses (1 copy)

CONTRACT/GRANT NUMBER:

REPORT TITLE:

is forwarded for your information.

SUBMITTED FOR PUBLICATION TO (applicable only if report is manuscript):

Sincerely,

A. M. Mellor, Ph.D.
Centennial Professor of Mechanical Engineering
Vanderbilt University

REPORT DOCUMENTATION PAGE

Form Approved
OMB NO. 0704-0188

1. AGENCY USE ONLY (Leave Blank)	2. REPORT DATE	3. REPORT TYPE AND DATES COVERED
	6/11/03	Final Report, 7/1/98-6/30/03

4. TITLE AND SUBTITLE
DI Diesel Performance and Emissions Models

5. FUNDING NUMBERS
DAAG55-98-I-0433

6. AUTHOR(S)
Mellor, A. M. and Easley, W. L.

7. PERFORMING ORGANIZATION NAME(S) AND ADDRESS(ES)
Vanderbilt University
512 Kirkland Hall
Nashville, TN 37240

8. PERFORMING ORGANIZATION REPORT NUMBER

9. SPONSORING / MONITORING AGENCY NAME(S) AND ADDRESS(ES)
U. S. Army Research Office
P.O. Box 12211
Research Triangle Park, NC 27709-2211

10. SPONSORING / MONITORING AGENCY REPORT NUMBER
P-37555.9-EG

11. SUPPLEMENTARY NOTES
The views, opinions and/or findings contained in this report are those of the author(s) and should not be construed as an official Department of the Army position, policy or decision, unless so designated by other documentation.

12 a. DISTRIBUTION / AVAILABILITY STATEMENT
Approved for public release; distribution unlimited.

12 b. DISTRIBUTION CODE

13. ABSTRACT (Maximum 200 words)

Development of models for direct injection diesel performance and emissions of NO_x and soot are the goals of this research. The simplest models investigated are flame temperature correlations. These correlations are semi-empirical tools that provide insight into the effects of dilution on NO_x, particulate, and HC emissions and can be used by the design or calibration engineer to reduce the number of engine tests required. A characteristic time model for NO_x emissions has been used to study the mixing processes in diesel engines and extended to study multiple injections, water/steam dilution, and the results of NO injection tests. This NO_x model was also modified to calculate the NO formed in the cylinder as a function of time and was shown to correlate engine-out NO_x emissions for four diesel engines. Development of a cycle simulation code is also underway. Primary emphasis has been placed on the study of the ignition and combustion submodels for this code. The NO_x model mentioned above has been included in the code and a soot submodel proposed. Upon completion, the cycle simulation code will allow evaluation of new schemes for improving performance, power density, and pollutant emissions.

14. SUBJECT TERMS
diesel, combustion, emissions, NOx, soot, ignition, emissions correlations, thermal ignition theory, homogeneous charge compression ignition, characteristic time modeling, NO injection, multiple injections, cycle simulation

15. NUMBER OF PAGES
46

16. PRICE CODE

17. SECURITY CLASSIFICATION OF REPORT	18. SECURITY CLASSIFICATION ON THIS PAGE	19. SECURITY CLASSIFICATION OF ABSTRACT	20. LIMITATION OF ABSTRACT
UNCLASSIFIED	**UNCLASSIFIED**	**UNCLASSIFIED**	**UL**

DI Diesel Performance and Emissions Models
ARO Grant # DAAG55-98-I-0433

A. M. Mellor and W. L. Easley
Vanderbilt University

June 11, 2003

Table of Contents

	Page
Table of Contents	ii
Nomenclature	iv
List of Figures	viii
List of Tables	x
1.0 Introduction and Statement of the Problems Studied	1
2.0 Flame Temperature Correlation of Emissions	2
2.1 Background	2
2.2 Statement of the Problem Studied	2
2.3 Summary of the Most Important Results	2
3.0 Quasi-static Characteristic Time Model for NO_x Emissions	3
3.1 Background	3
3.2 Statement of the Problem Studied	5
3.3 Summary of the Most Important Results	5
4.0 NO Injection Tests and Analysis Using the NO_x Characteristic Time Model	5
4.1 Background	5
4.2 Statement of the Problem Studied	5
4.3 Summary of the Most Important Results	5
5.0 Multiple Injection Tests and Analysis Using the NO_x Characteristic Time Model	6
5.1 Background	6
5.2 Statement of the Problem Studied	7
5.3 Summary of the Most Important Results	7
6.0 Water/Steam Dilution Tests and Analysis Using the NO_x Characteristic Time Model	7
6.1 Background	7
6.2 Statement of the Problem Studied	8
6.3 Summary of the Most Important Results	8
7.0 Dynamic NO_x Model	8
7.1 Background	8
7.2 Statement of the Problem Studied	9
7.3 Summary of the Most Important Results	9
8.0 Homogeneous Charge Compression Ignition Models	10
8.1 Background	10
8.2 Statement of the Problem Studied	10

8.3 Summary of the Most Important Results 10

9.0 Cycle Simulation Code Development 12
9.1 Background 12
9.2 Statement of the Problem Studied 12
9.3 Summary of the Most Important Results 12

10.0 Ignition Model Development 14
10.1 Background 14
10.2 Statement of the Problem Studied 15
10.3 Model Description 16
10.3 Summary of the Most Important Results 16

11.0 Combustion Model Development 17
11.1 Background 17
11.2 Statement of the Problem Studied 19
11.3 Model Description 19
11.4 Summary of the Most Important Results 25

12.0 NO_x Model Development 25
12.1 Background 25
12.2 Statement of the Problem Studied 29
12.3 Summary of the Most Important Results 29

13.0 List of All Publications and Technical Reports 30

14.0 List of All Participating Scientific Personnel Showing Any Advanced Degrees 31

15.0 Report of Inventions 31

Bibliography 32

Nomenclature

a - fuel reaction order

A - model constant; area; air

ATDC - after top dead center

b - oxidizer reaction order

BDC - bottom dead center

C_p - constant pressure specific heat

CAD - crank angle degrees

CTM - characteristic time model

CVB - constant volume bomb

d - diameter

D - angular momentum dissipation

DI - direct injection

E - activation energy

EGR - exhaust gas recirculation

EI - emissions index

EOC - end of combustion

EOI - end of injection

EVO - exhaust valve opening

F - fuel

h_{fg} - enthalpy of vaporization

H - flame lift-off height

HC - hydrocarbon

HCCI - homogeneous charge compression ignition

HSDI - high speed direct injection

IMEP - indicated mean effective pressure

ISFC - indicated specific fuel consumption

IVC - intake valve closing

L - liquid fuel length

m - mass

n - moles; model constant

P - pressure; angular momentum production

PFI - port fuel injection

Q_{LHV} - fuel lower heating value

R - ideal gas constant; radius; flame lift-off height in model

RPM - revolutions per minute

s_L - laminar flame speed

S - spray plume penetration length

SOI - start of injection

SI - spark ignition

SOC - start of combustion

t - time

T - temperature

TDC - top dead center

u' - global turbulence level

U - velocity

V - volume

x - distance between injector and premixed flame; mole fraction

δ_t - Taylor scale

ϕ - equivalence ratio

ρ - density

τ - characteristic time

ω - angular velocity

Ω - angular momentum

Subscripts

1 - zone 1

av - available

A - apparent

b - burned

c - chemical

ch - charge

cv - closed valve

cyl - cylinder

db - diffusion burn

e - eddy

en - entrained

f - fuel

fl - flame

id - ignition delay

init - initial

inj - injection

mix - mixing

pb - premixed burn

res - residence

sd - standard air

sp - spray plume

sq - squish

sw - swirl

util - utilization

x - at location of premixed flame

$\phi = 1$ - stoichiometric conditions

Other

[] - concentration

$\bullet$ - rate

List of Figures

		Page
1.	Schematic of the two-zone model for NO formation and decomposition in a DI diesel combustion chamber (Mellor et al., 1998a).	4
2.	Flow chart of simulation process. The models that are discussed in the following sections have the section number included.	13
3.	Schematic of a fully developed combusting fuel plume based on work of Dec (1997) and Flynn et al. (1999). Typical values of important lengths and temperatures achieved during diesel combustion have been included.	18
4.	Schematic of a bowl-in-piston combustion chamber showing squish flow and the large-scale eddy envisioned by Schihl (1998).	20
5.	Schematics of the DI diesel spray plume (a) at SOC, (b) a short time after SOC, and (c) later in the combustion event when the premixed flame has reached its steady-state location. Gray is used for vapor fuel, with darker shades indicating richer mixtures. Blue lines mark the location of the premixed flame and green lines the location of the diffusion flame. Red shows the products of premixed combustion with lighter shades indicating higher temperatures.	22
6.	Schematics of the DI diesel spray plume (a) just prior to EOI, (b) a short time after EOI, and (c) after all of the fuel has passed through the premixed flame but before EOC. Gray is used for vapor fuel, with darker shades indicating richer mixtures. Blue lines mark the location of the premixed flame and green lines the location of the diffusion flame. Red shows the products of premixed combustion with lighter shades indicating higher temperatures.	24
7.	The rates (a) and masses (b) of fuel injected ($m_{f,inj}$), fuel entrained in the premixed flame ($m_{f,en}$), fuel consumed in by the premixed flame ($m_{f,pb}$), fuel consumed in the diffusion flame ($m_{f,db}$), and total fuel burned ($m_{f,b}$) for the operating condition shown in Table 2. The legend in (a) applies to (b) as well.	26
8.	Figure 8: Comparison of the experimental and predicted (a) apparent rate of heat release and (b) cylinder pressure for the operating condition shown in Table 2.	27
9.	The closed valve indicated mean effective pressure ($IMEP_{cv}$) calculated from the experimental cylinder pressure data versus that calculated with the cycle simulation code. The dashed line has a slope of one and	28

indicated perfect prediction. The solid line is a best-fit to the data with fit statistics given provided on the graph. The red datum is for the operating condition in Table 2.

List of Tables

		Page
1.	Some important works examining fuel spray ignition delay using Eq. (2) or (3). All but the last three works are for diesel fuels. The last three works presented are for different fuels injected using a diesel type injector.	15
2.	0.75 L single-cylinder DI diesel engine operating conditions for which sample results are shown in Fig. 7 and 8.	25

1.0 Introduction

The goal of this work has been to develop models for the prediction of direct injection (DI) diesel engine performance and emissions of NO_x and soot. To aid in accomplishing this goal, a program review panel consisting of key personnel from the Army, academia, and industry was formed at the inception of this program in order to ensure cooperation and enhance collaboration between the various interested parties and users of technology to be developed under this program. Some of the institutions that have funded engine tests, supplied data or simulation tools, or provided technical information are Ford Motor Company, Caterpillar Inc., Cummins Inc., U. S. Army TACOM, and the University of Wisconsin-Madison. The support of these institutions is greatly appreciated.

The focus of the program has shifted several times in order to examine topics of interest to these many different intellectual sponsors. The topics examined include:

- Flame Temperature Correlation of Emissions
- Quasi-static Characteristic Time Model for NO_x Emissions
- NO Injection Tests and Analysis Using the NO_x Characteristic Time Model
- Multiple Injection Tests and Analysis Using the NO_x Characteristic Time Model
- Water/Steam Dilution Tests and Analysis Using the NO_x Characteristic Time Model
- Dynamic NO_x Model
- Homogeneous Charge Compression Ignition Engine Models
- Cycle Simulation Code Development
- Ignition Model Development
- Combustion Model Development
- NO_x Model Development
- Soot Model Development

A brief background, a statement of the problem studied, and a summary of the most important results are given for each of the above topics in the following sections. Only the most important technical details are provided in each section as publications regarding each topic are available and have been submitted to the Army Research Office through the appropriate channels. The exceptions are Sections 9.0 - 13.0 on the cycle simulation code and the submodels being developed for this code. Results of these studies have yet to be published and therefore greater detail is provided in these sections.

Note that many of the topics examined are related to NO_x emissions. Current Army propulsion systems are not restricted in the amount of NO_x they may emit, but by analyzing the mixing processes in the cylinder during NO formation and decomposition, information relevant to the whole combustion process may be obtained. These models can then be used to gain insight or to aid the design engineer in determining the best engine design to achieve good air utilization (high power density). Also, as discussed in Easley and Mellor (2002a), the original power density modeling concept centered on correlating power density to NO_x emissions. If this correlation could be developed, then by using the quasi-static NO_x models (see Section 3.0), the power density for a given engine condition could be evaluated. Difficulties in correlating power density to NO_x emissions for a wide range of operating conditions led to this model being abandoned for a more direct approach, a cycle simulation type code (see Section 9.0).

2.0 Flame Temperature Correlation of Emissions

2.1 Background

Work by Plee, Ahmad, and coworkers in the 1980s (Ahmad and Plee, 1983; Ahmad et al., 1982; Plee et al., 1981a; Plee et al., 1981b; Plee et al., 1982) showed that for changes in intake air state, diesel NO_x, soot, soluble organic fraction, and HC emissions could be correlated using the stoichiometric flame temperature calculated at start of combustion (SOC) or peak pressure conditions. Their model equation has the form

$$\ln \frac{EI}{EI_{sd}} \propto \pm \frac{E}{R}\left(\frac{1}{T_{\phi=1}} - \frac{1}{T_{\phi=1,sd}} \right) \tag{1}$$

where EI and $T_{\phi=1}$ are the emissions index and stoichiometric flame temperature for engine operation with various intake air compositions and EI_{sd} and $T_{\phi=1,sd}$ are the emissions index and stoichiometric flame temperature for engine operation with standard air. The stoichiometric flame temperature was calculated at either start of combustion or peak pressure conditions. E is the activation energy and R the ideal gas constant. Using results of engine tests in which the intake charge composition was altered either by diluent addition or oxygen enrichment (alters the flame temperatures) and graphing the left-hand side of Eq. (1) versus the term in parentheses on the right, a straight line results with the slope being the activation temperature (E/R).

Plee, Ahmad, and coworkers were successful in obtaining what at that time appeared to be a global activation temperature of ~35,000 K for NO_x emissions. This activation temperature was thought to be global because it correlated NO_x emissions for all four of the engines tested by the investigators. Engine dependent activation temperatures were also obtained for particulate, soluble organic fraction (or volatiles), soot, and HC.

2.2 Statement of the Problem Studied

The present work focused on obtaining correlations similar to those of Plee, Ahmad, and coworkers (Ahmad and Plee, 1983; Ahmad et al., 1982; Plee et al., 1981a; Plee et al., 1981b; Plee et al., 1982) for emissions of NO_x, particulate, and HC for three test engines; a 1.2 L high speed DI (HSDI) diesel, a 2.4 L HSDI diesel, and a 2.34 L single-cylinder DI diesel engine, the first of which was tested using four alternative fuels. The 1.2 L and 2.4 L engine tests were conducted at Ford Motor Company and Caterpillar Inc., respectively. In these tests exhaust gas recirculation (EGR) was used to change the intake air state and thus the stoichiometric flame temperature. The 2.34 L engine tests were conducted at the University of Wisconsin - Madison and used water fumigation (Foster, 1997). The primary objective was to determine if the same NO_x activation temperature obtained by Plee, Ahmad, and coworkers applies to modern DI diesels. Second, the authors wanted to conclude if engine dependent correlations of particulate and HC were feasible for modern DI diesels. Another objective was to resolve if these correlations could be applied to alternative diesel fuels as well.

2.3 Summary of the Most Important Results

The results show that diluent addition effects on NO_x emissions for each engine can be correlated using the SOC or peak pressure stoichiometric flame temperature, either of which gives the same activation temperature result. However, each engine examined had a somewhat different activation temperature. The activation temperature for the engine tested with

alternative fuels was found to correlate NO_x emissions for all the fuels tested. Further, the activation temperatures determined in the present study were found to be significantly higher than that of Plee, Ahmad, and coworkers (Ahmad and Plee, 1983; Ahmad et al., 1982; Plee et al., 1981a; Plee et al., 1981b; Plee et al., 1982). The differences in activation temperatures for each engine were concluded to be due to the effects of diluent addition on the combustion process, which were not captured through the use of a single theoretical temperature.

Particulate and HC emissions were also correlated using the SOC and peak pressure stoichiometric flame temperatures. However, for these emissions activation temperature was found to depend upon the choice of characteristic temperature (SOC or peak pressure stoichiometric flame temperature in this study). Further, activation temperature was also found to be a function of operating condition. The separate correlations for each operating condition are thought to arise due to the use of only a characteristic temperature to account for the oxidation of the particulate and HC. As diluents are added the formation is affected as well. The alternative fuel results show that at each operating condition a reasonable correlation exists for the HC emissions from the alternative fuels, but that the particulate emissions from the different fuels tests exhibit different temperature dependencies, a result most likely occurring from the different aromatic contents of the fuels.

Correlations of this type are valuable for many reasons. Though this model is quite simple, it provides information about the emissions forming processes in the engine. Most importantly, these correlations provide the test engineer with insight that can aid in designing engine tests as well as reduce the number of tests that are needed. For example, to determine the effects of EGR on NO_x, HC, and particulate emissions for a given operating condition (speed, load, injection pressure, etc.), only this operating condition without EGR and this same operating condition with some arbitrary amount of EGR addition need be tested. From these data an activation temperature for each emission can be determined and the emissions for this operating condition with other EGR rates calculated. Further details on this work may be found in Easley et al. (2001b).

3.0 Quasi-static Characteristic Time Model for NO_x Emissions

3.1 Background

The global NO reaction activation temperature found by Plee et al. (1981b) of ~35000 K (see Section 2.1) is much lower than that for NO formation through the extended Zeldovich mechanism (Lavoie et al., 1970) kinetics (~69000 K). Plee et al. (1981b) conclude that the reason for the lower activation temperature is that NO decomposition is also important. Based on this finding, Mellor et al. (1998a), funded by ARO grant #DAAH04-94-G-0236, proposed a two-zone quasi-static characteristic time model (CTM) that accounts for both NO formation and decomposition explicitly. NO forms in the first zone, which is characterized by the stoichiometric flame temperature calculated at SOC conditions, and may decompose in the second zone, which is characterized by the end of combustion (EOC) bulk temperature computed from a fuel/air limited-pressure cycle analysis. A schematic of this model is shown in Fig. 1. In the two-zone model the global reaction used by Plee et al. (1981b) is replaced by a skeletal mechanism that includes both extended Zeldovich (Lavoie et al., 1970) and nitrous oxide (Malte and Pratt, 1974) kinetics (Mellor et al., 1998a). A detailed model description is provided by Mellor et al. (1998a) and Mellor et al. (1998b).

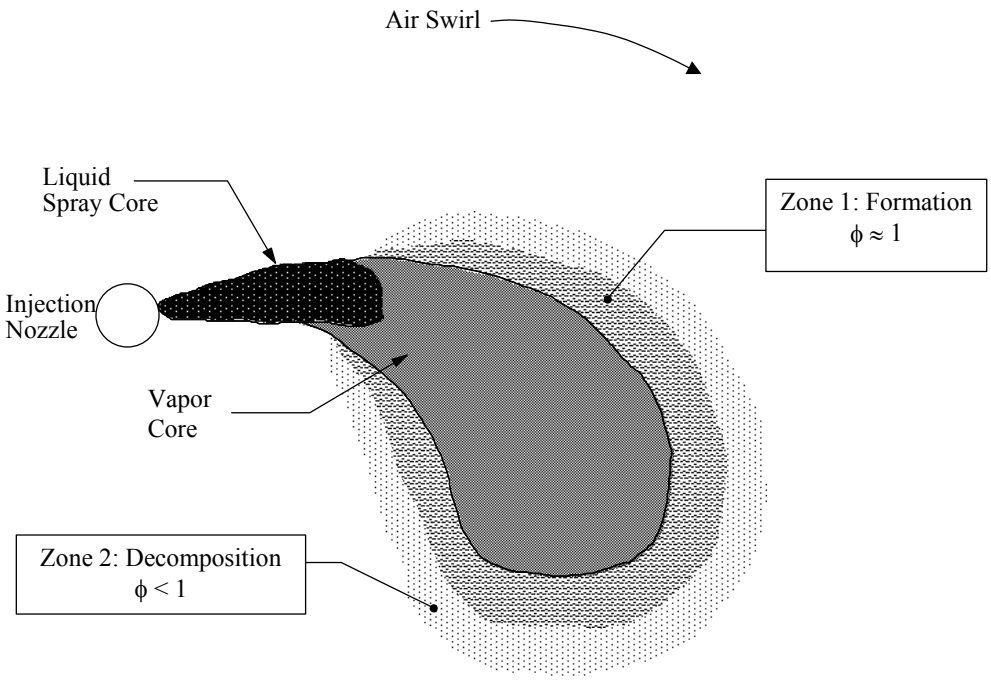

Figure 1: Schematic of the two-zone model for NO formation and decomposition in a DI diesel combustion chamber (Mellor et al., 1998a).

3.2 Statement of the Problem Studied

The primary goals of the work conducted on this model under this grant were to develop the fluid mechanic aspects of the model and validate the model with engine data. To achieve these goals, 2.2 L HSDI diesel engine tests were conducted at Ford Motor Company and the data used for model development and validation. The data consist of exhaust gas recirculation variations from zero to maximum level possible for parametric variations of engine speed, injection pressure, and load.

3.3 Summary of the Most Important Results

The NO_x CTM was validated using the data from the 2.2 L HSDI diesel engine. An expression for the characteristic mixing time, which accounts for the fluid mechanic mixing effects on NO_x emissions, was developed that is a function of the charge Reynolds number, liquid phase fuel Weber number, injection velocity, and engine geometry. The characteristic mixing time was then used in the NO_x CTM to correlate NO_x emissions for conditions in which NO decomposition is negligible. A method of evaluating at which conditions NO decomposition is negligible, originally proposed by Mellor et al. (1998a), was also validated. Further details on this work may be found in Duffy and Mellor (1998) and Duffy (1998).

4.0 NO Injection Tests and Analysis Using the NO_x Characteristic Time Model

4.1 Background

The works of Mellor et al. (1998a) and Duffy and Mellor (1998) conducted under this and a previous ARO contract indicated that NO decomposition occurs in diesel engines and becomes more important as load is increased. The results of engine modeling (Blumberg and Kummer, 1971; Plee et al., 1981b), cylinder dumping experiments (Voiculescu and Borman, 1978), and NO injection tests (Aiman, 1973; Plee et al., 1981b) reported in the literature also support the finding that NO decomposition is important in piston engines (for an in-depth discussion of these works see Easley and Mellor (1999)). Despite these indications that NO decomposition is important in the DI diesel engine, a careful systematic study had not been conducted prior to this work to quantify the importance of NO decomposition in DI diesels or fully understand the process by which it decomposes.

4.2 Statement of the Problem Studied

Two goals of this work were to determine a method of evaluating the importance of NO decomposition in DI diesel engines and to determine how changes in operating conditions, such as engine load and speed, affect NO decomposition. These goals were accomplished through NO injection experiments conducted at Caterpillar Inc. on a 2.4 L HSDI diesel engine. The tests are described in more detail below. Further, the NO_x CTM of Section 3.0 was modified for use with these tests. Use of the model in combination with the NO injection data allowed several important aspects of the model to be evaluated. Further, the model allowed the amount of NO decomposition at each operating condition to be quantified.

4.3 Summary of the Most Important Results

NO decomposition in DI diesel engines was explored using data from a 2.4 L HSDI diesel engine in which pure NO was added to the intake air in various amounts and the resulting

exhaust concentrations of NO and NO_x measured. Data of this type were taken for a load sweep and a speed sweep. NO injection results obtained by Aiman (1973) on a SI engine and Plee et al. (1981b) on an indirect injection (IDI) diesel were also examined. A common conclusion is that the importance of NO decomposition increases with equivalence ratio for all three types of engines, but the amount of decomposition depends on the burn phasing and cycle design, as expected.

Engine-out NO and NO_x were found to be linear functions of engine-in NO for all data, indicating that the mechanism responsible for NO decomposition is first order with NO. The reverse Zeldovich mechanism (first order with NO) is therefore the dominant mechanism for NO decomposition. Analysis of the 2.4 L HSDI diesel engine data revealed that engine-out NO_2 increases non-linearly with engine-in NO, but the origins of this result are uncertain. The NO_2 may have formed in the engine cylinder or in the exhaust stack, probe, or analyzer line before the exhaust concentrations were measured. Because of the relatively small concentration of NO_2, the engine-out NO_x emissions could also be approximated to increase linearly with NO injection.

The NO_x CTM described in Section 3.0 was modified for use with these tests. Recall that the NO chemistry in this model includes the extended Zeldovich mechanism (Lavoie et al., 1970) and important reactions from the nitrous oxide mechanism (Malte and Pratt, 1974). Results of the analysis reveal that both the extended Zeldovich and nitrous oxide mechanisms are important for NO formation with Zeldovich faster at normal diesel operating conditions and nitrous oxide becoming more important as diesel flame temperatures are lowered by diluent addition (EGR or water). Only the reverse Zeldovich chemistry is found to be important for NO decomposition.

Further, in the NO_x CTM NO forms in zone 1 and may decompose in zone 2. The form of the model equations allows the residence time in each zone to be evaluated using the results of the NO injection tests. The residence time results indicate that the bulk EOC temperature as model temperature for zone 2 cannot simulate the actual situation. Rather, NO decomposition must occur in a zone defined by an equivalence ratio closer to one.

The amounts of NO formed and decomposed can also be calculated using the model equations. At 2000 RPM NO decomposition is found to increase from 6% at the lightest load tested (~ 15% full load) to 37% at the highest load (95% full load). NO decomposition is also found to exhibit a tradeoff with engine speed. The peak percentage of decomposition for the speed sweep (conducted for a BMEP of 800 kPa) is approximately 32% and occurs at 1500 RPM, the lowest speed tested. However, these estimates depend on the present model assumptions.

Additional information on the NO injection tests and other tests examining NO decomposition reported in the literature can be found in Easley and Mellor (1999) and Easley (2000). Discussion of the analysis of the NO injection data using the NO_x CTM is provided in Easley et al. (2000) and Easley (2000).

5.0 Multiple Injection Tests and Analysis Using the NO_x Characteristic Time Model

5.1 Background

A CTM for NO_x emissions was derived by Mellor et al. (1998a), validated by Duffy and Mellor (1998), and subsequently modified by Easley et al. (2001) as discussed in Sections 3.0 and 4.0. However, this CTM was developed for use with single injections and SOC at top dead center (TDC) only. Start of combustion timing is typically optimized to achieve the best

emissions and fuel economy possible and thus does not always occur at TDC. Further, modern DI diesel engines often use multiple injections to control emissions of NO_x and soot while maintaining good fuel economy.

5.2 Statement of the Problem Studied

The CTM for NO_x emissions was modified in order to model the effects of SOC timing and multiple injections. NO_x emissions data from a 1.2 L HSDI diesel engine tested at Ford Motor Company using multiple injections and EGR for emissions control were then analyzed with the model in order to determine how SOC timing and multiple injections affect NO_x emissions and to validate the model for the prediction of NO_x emissions under these conditions.

5.3 Summary of the Most Important Results

The analysis of multiple injections using the NO_x CTM provided insight into how the injection scheme affects engine-out NO_x emissions. Good agreement between model predictions and experimental data confirmed the model postulate that retarded injection timing and EGR lower the stoichiometric flame temperature, and thus depress the chemical rates of NO formation. The characteristic fluid mechanic time for NO formation can be shortened relative to a conventional single injection by utilizing a lower initial injection rate in a double injection, which results in lower injection velocity and decreases NO_x emissions from DI diesel engines. The model also shows that emissions of NO_x are linearly proportional to fuel quantity for each injection pulse per injection event.

The effect of EGR on NO_x emissions with post injection was also confirmed by this model. At different EGR rates, multiple injections have different effects on NO_x emissions. Multiple injections at lower EGR rates provide enhanced NO_x emissions reduction. However, EGR plays a more significant role in NO_x reduction than do any of the multiple injection schemes examined. The model demonstrates that this result is explained by the exponential Arrhenius temperature dependence of the chemistry.

The analyses in this research work have extended the NO_x characteristic time model to multiple injections for DI diesel engines. However, this work has limitations. First, due to the limited information available for the injector utilized, the cumulative heat release curve for a given engine test must be used to deduce the fraction of fuel burned in each injection pulse. Second, the normalization of the data as used here provides insight only into the relative effects of different parameters, and the single injection emissions are needed as baseline data. If NO_x predictions for single injections are available from other simulation tools, then the relative NO_x reduction of multiple injections can be calculated by using the CTM modeling method introduced in this research. Additional details on this research are provided in Yang et al. (2002) and Yang (2002).

6.0 Water/Steam Dilution Tests and Analysis Using the NO_x Characteristic Time Model

6.1 Background

Introduction of an inert diluent into the cylinder of a diesel engine is one method that is often used to reduce NO_x emissions. The most common diluents used are exhaust gases and steam/water. These diluents act to decrease the oxygen concentration in the charge and increase the specific heat of the charge, both of which decrease the flame temperatures in the engine

thereby decreasing NO formation. For the case of liquid water injection into the cylinder the flame temperatures are further reduced due to the heat of vaporization of the water.

6.2 Statement of the Problem Studied

The NO_x CTM discussed in previous sections is extended to the cases of water or steam dilution. Data are available for direct water injection and steam dilution. Kohketsu et al. (1996) directly inject water into the cylinders of an 11.2 L Mitsubishi DI diesel engine using a specially designed injection system. Foster (1997) conducted steam fumigation (supplied to intake manifold) studies on a 2.34 L single-cylinder research DI diesel engine. The comparison of the NO_x CTM to measured NO_x emissions provides insight into the role of inert diluents in reducing NO_x emissions from DI diesel engines. Specifically, the CTM is used to compare the effectiveness of different water distribution techniques.

6.3 Summary of the Most Important Results

Analysis of the Kohketsu et al. (1996) data reveals that the NO_x reduction potential associated with direct water injection is over 90% for the non-practical situation in which all of the water enters stoichiometric eddies (NO formation zone). As indicated by the measured NO_x data, however, the actual reduction through this technique is slightly less than 90 % at the highest water-to-fuel mass ratio tested. In fact the comparison between the data and the model indicates that the fraction of water entering stoichiometric eddies increases as the water-to-fuel mass ratio is increased.

A similar analysis of NO_x reduction through intake manifold fumigation shows that steam is in this case uniformly distributed in the cylinder at SOC, as expected. Qualitatively, this aspect of the study demonstrates that a reduction in NO formation is effected by retarding the fuel injection timing and increasing the engine load at a given engine speed. The former observed means of NO reduction is a fluid mechanic effect, while the source of reduction through the latter remains uncertain given the current unavailability of injection rate profile information for these data.

Methodologies for both qualitatively and quantitatively assessing the importance of NO decomposition in engines at different operating conditions are also established. The work performed here extends to the reduction of NO_x using other types of diluents. Using similar methodology, EGR results have been analyzed by Duffy and Mellor (1998). Further details on this work are provided in Mello and Mellor (1999) and Mello (1998).

7.0 Dynamic NO_x Model

7.1 Background

In Sections 3.0 - 6.0 development, validation, and use of the quasi-static NO_x CTM have been discussed. In that model the NO formation in zone 1 is characterized by a single theoretical temperature, the stoichiometric flame temperature at start of combustion conditions. The NO decomposition process is also characterized by a single theoretical temperature, the bulk EOC temperature calculated using the limited pressure cycle. By using a single theoretical temperature for each process the engine-out emissions may be written as an algebraic equation. Because of its simple form, this model is a valuable tool for gaining insight into the NO formation and decomposition processes and has been shown to correlate NO_x emissions over

limited ranges of engine operating conditions (Duffy and Mellor, 1998; Yang and Mellor, 2002). However, in simplifying the problem many of the secondary details of the combustion and emissions formation processes are lost.

7.2 Statement of the Problem Studied

In an effort to conduct a more detailed analysis, the skeletal mechanism for NO_x chemistry proposed by Mellor et al. (1998a) is incorporated in an engine simulation code. The two-zone model, also proposed by Mellor et al. (1998a), is modified for use in the simulation code. Based on the results a one-zone model is also explored, but does not correlate the available engine data as well as the two-zone model. The simulation code is zero-dimensional, with bulk and stoichiometric flame temperatures and fuel-burning rate calculated at each crank angle degree from cylinder pressure time histories. The model is compared with data from four heavy-duty DI diesel engines.

7.3 Summary of the Most Important Results

Following the work of Mellor et al. (1998a), the two-zone model is postulated to consist of a zone where NO formation occurs and a separate zone where the decomposition of NO proceeds. For the formation zone, the stoichiometric flame temperature and corresponding species concentrations are used, while the bulk cylinder temperatures and concentrations represent NO decomposition. Results indicate that both the Zeldovich and N_2O mechanism contribute to the total NO formed; furthermore, as the peak flame temperatures are reduced, through the use of EGR or retarded SOC timing, the relative importance of the N_2O mechanism increases, eventually becoming the dominant pathway for NO formation. Use of the bulk temperature to characterize zone 2 indicates NO decomposition is negligible.

Predicted engine-out NO_xEI values were compared to measurements for four heavy-duty DI diesels. A single correlating equation was found between the predicted and measured values for all engines, suggesting that the two-zone model appears to mimic NO kinetics for diesels. The observed overprediction of NO_xEI may arise from improper modeling of the stoichiometric volume of the diesel spray plume, overprediction of the stoichiometric flame temperature, or not considering equilibration of reaction (R5) ($O + N_2 + M \leftrightarrow N_2O + M$) in the two-zone model. Another possible cause may be including the NO kinetics associated with the N_2O mechanism, but a correlation restricted to the Zeldovich mechanism exhibits worsened statistics.

A one-zone flame model characterized by stoichiometric combustion was also evaluated, but a major difficulty arises: defining the amount of NO available for decomposition. Unlike the two-zone model, where it is assumed that all NO formed immediately enters the decomposition zone, in the one-zone application some NO may exit the zone without participating in decomposition. Various possibilities of the definition for the NO available for decomposition were examined. It was found that none provides correlations as good as those for the two-zone model. Due to the absence of mixing in a zero-dimensional simulation, it is recommended that the two-zone model, including both the Zeldovich and N_2O mechanisms, be applied for engineering purposes. Details of the model and analysis may be found in Psota and Mellor (2001) and Psota (2001).

8.0 Homogeneous Charge Compression Ignition Models

8.1 Background

The use of autoignition to initiate the combustion process in homogeneous charge engines has been known by many names in the past, but is now most commonly called homogeneous charge compression ignition or HCCI. The use of HCCI as a distinct, controlled engine operating mode was suggested over twenty years ago by Onishi et al. (1979) and Noguchi et al. (1979) for use in two-stroke gasoline engines. Initial studies using HCCI in four-stroke engines were conducted by Najt and Foster (1983). These authors concluded that the HCCI combustion process is controlled solely by chemical kinetics (mixing is insignificant to the combustion process) and that the heat release rate, though it shows little cycle-to-cycle variability, exhibits large changes depending on the operating conditions.

Engines operated in HCCI mode have the potential to provide better fuel economy and emissions than conventional SI engines. Emissions of soot (smoke) are very low because no rich regions where soot can form exist in the cylinder. Emissions of NO_x are also very low when HCCI is used at moderate to low speeds and loads (low equivalence ratios) because of low combustion temperatures. Unfortunately, CO and HC emissions are relatively high by today's standards. Further, HCCI operation is limited to moderate to low speeds and loads by combustion noise.

With HCCI operation, ignition is controlled solely by in-cylinder conditions. Perhaps the most studied method of achieving HCCI is the use of port fuel injection (PFI) to obtain a nearly homogeneous cylinder charge. Ignition timing may then be regulated by controlling the charge temperature and pressure using intake air conditioning, EGR, variable valve timing, variable compression ratio, or other methods. A similar method of achieving an almost homogeneous cylinder charge is the direct injection of fuel during intake or early in the compression stroke. Start of combustion can then be controlled in the same manner as when PFI is used.

8.2 Statement of the Problem Studied

The most attractive means of increasing the power density of present DI diesel engines is by increasing the fuel-to-charge ratio (Easley and Mellor, 2002a; BRC, 1995). The fuel-to-charge ratio in DI diesels is limited by soot or smoke emissions. Since no fuel rich regions exist in the cylinders of HCCI engines, smoke emissions are very low. Therefore, the potential exists for HCCI engines to operate at higher fuel-to-charge ratios than DI diesel engines. However, there are other factors that must be considered such as compression ratio, engine noise, durability, peak cylinder pressure constraints, whether the engine can perform in the harsh environments required by the U. S. Army, etc.

The present work focuses on the development of thermodynamic models coupled with detailed chemical kinetics for use in research and development of HCCI engines. These models are applicable to both PFI and early direct injection modes of operation and are based on experimental findings presented in the literature.

8.3 Summary of the Most Important Results

Single and multi-zone models for use in modeling the compression and expansion strokes of an HCCI engine were formulated. Either of these models could be incorporated into or used with a cycle simulation code to provide a complete model of the four-stroke cycle for HCCI

engine operation. In this work the models were used to simulate HCCI combustion in a representative passenger car/light truck type engine with a compression ratio of 15:1.

The single-zone model, representative of the adiabatic core region of the cylinder charge, was used to calculate the in-cylinder BDC temperatures needed in order to achieve SOC at TDC for a variety of operating conditions and fuels (iso-octane, n-heptane, methane, simulated gasoline - 13% n-heptane/87% iso-octane). The in-cylinder temperatures just prior to SOC were also reported. These results indicate that the control system for the HCCI engine need not vary the intake temperatures tremendously. The exact temperature range that the system will have to provide will be dependent on the load and speed range over which HCCI is used, the compression ratio of the engine, and the fuel used. Results were obtained for changes in load, speed, and fuel at a fixed compression ratio of 15:1.

NO_xEI was also computed for the same operating conditions and fuels using the single-zone model. NO was found to form in a very short period of time during the combustion process with almost zero NO decomposition observed following the formation period. Conversion of NO to NO_2 was found to be negligible for equivalence ratios greater than or equal to 0.2. For an engine speed of 2500 RPM and no intake boosting, the engine simulated was found to meet TIER II NO_x emissions standards for equivalence ratios of 0.3 and less. However, these results are for operation with pure air. Exhaust gas recirculation and SOC timing retard were not considered, but are expected to significantly reduce NO_x emissions and combustion noise, thus allowing engine operation at even higher equivalence ratios. NO_xEI simulation results from the single-zone model are also expected to be somewhat high due to the temperature homogeneity and adiabatic cylinder charge assumptions in the single-zone model.

The multi-zone model was formulated to include the effects of the boundary layer and crevice volume as well as to incorporate the effects of temperature and fuel-air mixture stratification. The multi-zone model is therefore much more suitable for predicting realistic cylinder pressure histories and emissions of NO_x, CO, and HC.

Detailed multi-zone modeling was conducted for methane as fuel due to the long simulation times required for higher hydrocarbons. For the simulations conducted as part of this work the fuel was assumed to be distributed evenly throughout the cylinder. The results clearly show the physical processes occurring during the compression, combustion, and expansion periods. NO_x was found to form in the core regions where the temperatures were high. HC emissions resulted from unburned fuel in the crevice and boundary layer regions and fuel that left these regions late during the expansion stroke that did not get oxidized. The most interesting finding was that most of the CO emissions were formed from unburned fuel-air mixture flowing from the boundary layer and crevice zones into the higher temperature parts of the cylinder during the expansion stroke where they were partially oxidized to form CO.

The model was also used in a parametric study to examine the effects of some important operating parameters on performance and emissions. The results of these studies shed light on how certain operating parameters can affect emissions and performance. Further details on this work may be found in Easley et al. (2001a).

9.0 Cycle Simulation Code Development

9.1 Background

The original plan for modeling NO_x emissions was through the use of the quasi-static NO_x CTM. However, after thorough analysis of this model its limitations became apparent as discussed in Section 7.1. This led to the formulation of the dynamic NO_x model. The dynamic NO_x model requires the burn rate as a function of crank position as an input. This information can be derived from experimentally acquired cylinder pressure data or predicted using a model. Of course, for the dynamic NO_x model to be predictive a simulation code is required for predicting the burn rate.

The original concept for modeling power density was centered on correlating power density to NO_x emissions, which would be predicted using the quasi-static NO_x CTM. As discussed in Section 1.0, there were several problems associated with this concept. Therefore, a more direct approach to modeling power density is required.

9.2 Statement of the Problem Studied

The primary goal of this work is the development of a simulation model/code for the prediction of DI diesel performance (power density, fuel consumption, torque, etc.) and emissions of NO_x and soot. The model predicts the in-cylinder conditions as a function of crank position from intake valve closing (IVC) to exhaust valve opening (EVO). The performance characteristics and engine-out emissions are then derived from these computations. The model can be used to study methods of increasing power density and decreasing fuel consumption and emissions of NO_x and soot.

A 0.75 L single-cylinder research DI diesel engine equipped with a state-of-the-art piezo-electric common rail injection system was tested at Ford Motor Company to provide data for development and validation of the model. Eight control parameters are required to set an operating condition with this engine. They are: engine speed, intake charge temperature, intake charge pressure, exhaust pressure, EGR rate, injection pressure, injection quantity, and injection timing. A parametric study of these eight control parameters, consisting of 135 data, was conducted for one engine configuration. Several data are also available for two other engine configurations (different injector nozzle and piston design).

9.3 Summary of the Most Important Results

The ignition, combustion, NO_x, and soot models are the primary submodels in the overall simulation. Details on ignition, combustion, and NO_x models are provided in the following sections along with the most important results obtained for each. A soot model was also derived, but is still in the preliminary stages of development and so is not discussed here.

A flow diagram that contains all of the major functions that the simulation code must conduct is shown in Fig. 2. The simulation starts by calculating the in-cylinder conditions, meaning the thermodynamic state and the initial mixing rate needed for the combustion model (see Section 11.0). The initial conditions, such as pressure, temperature, composition of the charge, etc. at IVC are input by the user. After each time step the in-cylinder conditions are output to a file.

As the simulation continues to loop, calculating the in-cylinder conditions throughout the compression stroke, it checks for start of injection (SOI), which is input by the user. When the simulation detects SOI it begins to calculate the spray characteristics using the model of Naber

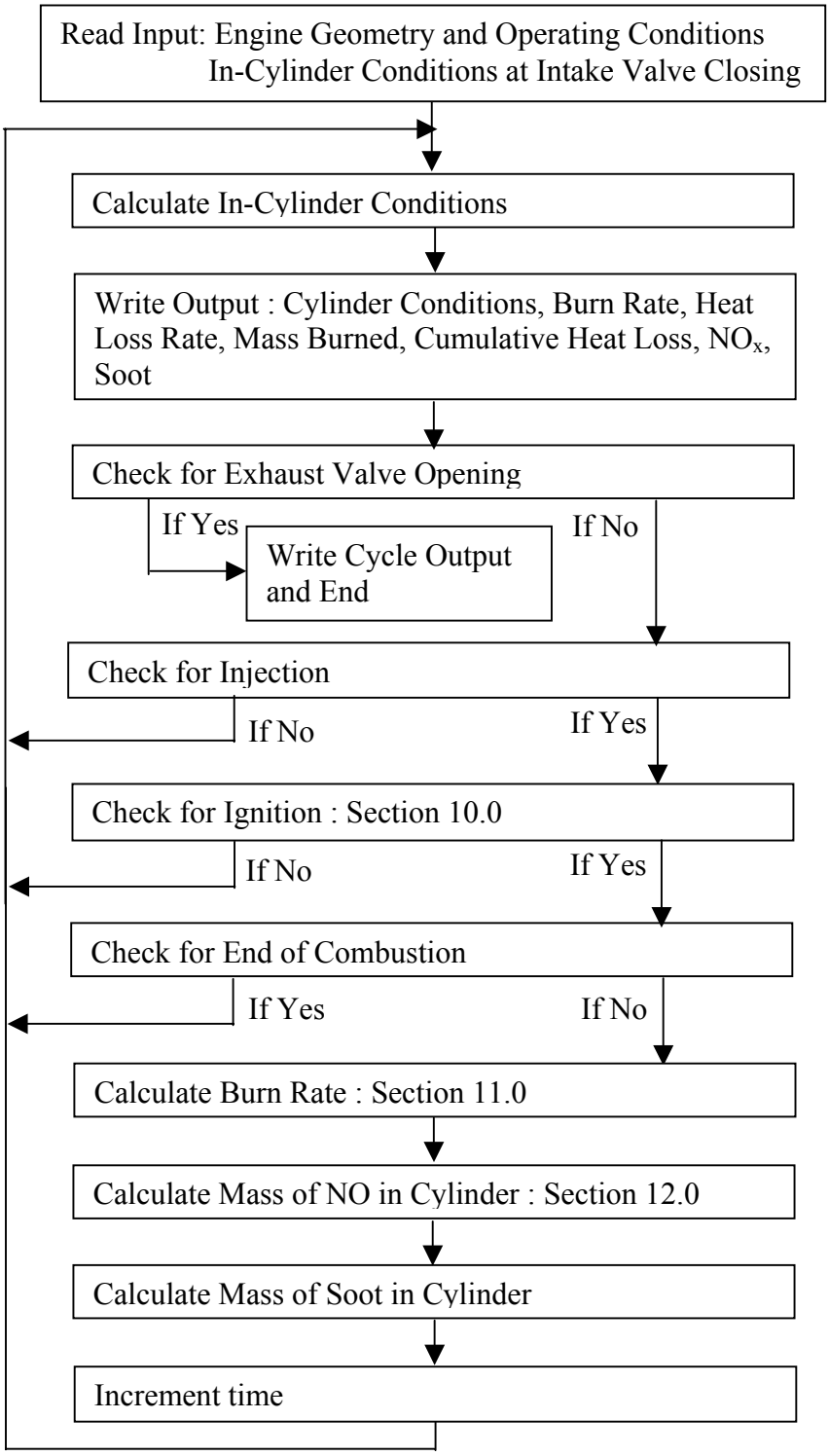

Figure 2: Flow chart of simulation process. The models that are discussed in the following sections have the section number included.

and Siebers (1996). The spray characteristics are needed for the ignition, combustion, NO_x, and soot model computations.

Upon SOI the ignition model is called at each time step to check for SOC. When the ignition model indicates that SOC has occurred the simulation initiates the combustion and emissions models. The combustion and emissions models continue to predict the burn rate and concentrations of NO_x and soot until the burn rate becomes negligible at which time the simulation ends the combustion and emissions formation events and continues to calculate the in-cylinder conditions throughout the expansion stroke. When EVO is reached the cumulative cycle outputs are calculated (IMEP, ISFC, engine-out NO_x, engine-out Soot, etc.) and printed to an output file.

The model is coded in C++ with the exception of the equilibrium solver STANJAN (Reynolds, 1995), which is used in the NO_x model (see Section 13.0). STANJAN (Reynolds, 1995) remains coded in FORTRAN 77 and is called from the main C++ program using functions available from Arnholm (1997), which allow FORTRAN 77 subroutines to be called from C++ by making the necessary conversions of data storage format for variables that are passed between the languages. C++ has been chosen because of its superior programming structure, easier handling of input and output, and its increasing popularity in engineering applications.

The ignition, combustion, and NO_x submodels are discussed in the following sections.

10.0 Ignition Model Development

10.1 Background

Wolfer (1938) was the first to study the ignition of diesel fuel sprays. He was able to correlate the ignition delay of a diesel fuel spray in a constant volume bomb (CVB) for different pressure and temperature conditions using an expression of the form,

$$\tau_{id} = A P_{ch}^{-n} \exp\left(\frac{E_A}{R T_{ch}}\right) \tag{2}$$

where A, n, and E_A are model constants and P_{ch} and T_{ch} are the vessel charge pressure and temperature during the ignition delay period.

In an engine the charge temperature and pressure change during the ignition delay due to piston motion (changing cylinder volume). One of two methods is typically used to apply Eq. (2) to diesel engines. First, the average temperature during the ignition delay period can be used as originally done by Bauer (1939). Second, the expression

$$\int_{SOI}^{SOI+\tau_{id}} \frac{1}{\tau}\, dt = 1 \tag{3}$$

can be employed, where τ is given by Eq. (2) for the temperature and pressure at time t, (Heywood, 1988).

Since Wolfer's work, many researchers have used Eq. (2) or (3) to correlate the ignition delay of fuel sprays. The ignition delay pressure and temperature dependencies, n and E_A/R, have values from 1.02 to 2.5 and from 1468 to 7813 K, respectively, for the studies examined. The wide range of values for these constants can be attributed to three factors:

1) The definitions or methods of determining SOI and SOC are different (Plee and Ahmad, 1983).
2) The fuels used are different.

3) The injector or method of fuel-air preparation (mixing) is different (Plee and Ahmad, 1983).

Of the three factors responsible for the wide range of model constant values, the effect of the fuel-charge mixing process is likely the greatest. Equation (2) has the form of an inverse reaction rate constant and thus only takes into account the chemical kinetic aspects of the ignition process. Since the effects of mixing are not included explicitly in the model equation, its effects are lumped into the chemical kinetic term and thus the constants determined for each test configuration account not only for the kinetic aspects of the fuel, but also the fuel-charge mixing processes. It is for this reason that the activation energy in Eq. (2) is referred to as an apparent activation energy (E_A).

The charge temperature and pressure are expected to affect the fuel-charge mixing process through their effects on charge density, which is the primary factor controlling spray-charge interaction (Naber and Siebers, 1996). However, the effects of pressure and temperature on the mixing process are accounted for, at least to some degree, by the pressure and temperature factors in Eq. (2). The model does not account for changes in mixing caused by such things as changing the injection system, injection pressure, or charge motion. For these types of changes the model must be recalibrated with experimental data.

Comparison of the activation temperatures reported in the literature for DI diesel fuel sprays (1468 - 7813 K) and those reported in the literature for various premixed hydrocarbon fuel-oxidizer systems (15851 - 29237 K) outside the negative temperature coefficient range of pressure and temperature reveals that the DI diesel fuel spray activation temperatures are much lower than those for premixed hydrocarbon fuel-oxidizer systems. Plee and Ahmad (1983) and Heywood (1988) conclude that lower values of the activation temperature in DI diesel fuel spray ignition models imply that mixing processes are important relative to chemical effects.

The results presented in this section reveal the main weakness of the Wolfer (1938) ignition model: the only way to determine the model constants is by calibration for each test configuration and/or fuel. Even when using the same fuel in two different engines, the model constants will be different due to the differences in the fuel-charge mixing process. Therefore, there is a need for a model that, while computationally simple, includes the effects of the mixing process explicitly. Formulation of such a model is the focus of this work.

10.2 Statement of the Problem Studied

The objective of this work is to develop and validate an ignition model for DI diesel sprays that incorporates explicitly the effects of mixing. Diesel spray ignition delay data from constant volume bomb (CVB) and DI diesel engine experiments are available for model development and validation. The CVB data have been supplied by Siebers (2002) from the work of Higgins et al. (2000). The DI diesel engine experiments were conducted using a 0.75 L single-cylinder DI diesel engine at Ford Motor Company as discussed in Section 9.0. Sample 0.75 L engine ignition delay results are presented by Easley and Mellor (2002b).

The ignition model is not only applicable to DI diesel sprays, but to any strained flow field. In order to validate the model for simple laminar flow fields and study the chemistry of diesel fuel and other higher hydrocarbon fuels, the results of counterflow (Seshadri, 2002) and liquid pool (Payer, 2002) tests, both having strained laminar flow fields, are being examined using the model. Application of the model to these tests allows the activation temperature (E/R) for the hydrocarbon fuels tested, one of which is diesel fuel, to be calculated.

10.3 Model Description

A potentially ignitable eddy is examined in order to determine the ignition timing. At the time of injection the eddy is composed entirely of liquid fuel at the fuel injection temperature. As the eddy penetrates into the cylinder it entrains charge and the fuel evaporates. The fuel eddy will continue to entrain charge, thereby increasing its temperature and oxygen concentration, until it eventually reaches conditions favorable for ignition.

Theoretically, the first eddy to be injected will be the first to ignite as it has the longest time to evaporate and mix with charge. This theoretical result is supported by images of diesel spray ignition in DI diesel engines (Dec, 1997) and in high-pressure vessels at conditions typical of DI diesels (Higgins et al., 2000; Edwards et al., 1992; Sato et al., 1986). Further, these experiments show that by the time of ignition all of the fuel in the ignition region has vaporized. Therefore the heat required for vaporization must be included in the model, but the evaporation process or rate is not of importance since it is known that the eddy will contain only vapor fuel at the time of ignition.

A first law of thermodynamics analysis of the eddy described above is conducted by Easley and Mellor (2002b). The analysis results in three equations,

$$\frac{dT_e}{dt} = \frac{A[\text{fuel}]^a[\text{oxid}]^b \exp(-E/RT_e)Q_{LHV}}{\rho_e C_{p,e}} - \frac{C_{P,e}T_e - C_{P,ch}T_{ch}}{\tau_{mix}C_{p,e}} - \frac{T_e}{C_{p,e}}\frac{dC_{P,e}}{dt} - \frac{R_e T_e}{C_{p,e}V_{ch}}\frac{dV_{ch}}{dt} + \frac{R_e T_e}{C_{p,e}V_{ch}T_{ch}}\frac{dT_{ch}}{dt} \quad (4)$$

$$n_{e,t} = n_{e,init} + \int_{SOI}^{t} \frac{n_e}{\tau_{mix}}\,dt \quad (5)$$

$$T_{e,t} = T_{e,init} + \int_{SOI}^{t} \frac{dT_e}{dt}dt - \frac{h_{fg}}{C_{p,e}} \quad (6)$$

which can be solved numerically along with the species conservation equations to determine the eddy rate of temperature rise and temperature and the number of moles in the eddy. The subscripts e and ch indicate eddy and bulk charge conditions, respectively. The remainder of the variable definitions is supplied in the nomenclature. The first term on the right hand side of Eq. (4) accounts for the effect of reaction on the eddy rate of temperature change. Note that a one-step reaction of fuel with oxidizer has been assumed. The second term on the right hand side accounts for the eddy temperature change as charge is entrained. The remaining three terms account for work done on the eddy as the cylinder volume changes. Ignition is said to occur when the kinetic term in Eq. (4) (first term on right hand side) becomes large.

10.4 Summary of the Most Important Results

The counterflow and liquid pool data were examined first in order to validate the model for a simple laminar flow field in which the mixing process is well characterized and to determine an appropriate activation temperature for diesel fuel. Mellor et al. (2003) use time-independent thermal ignition theory applied to these experiments and thus define an ignition criterion in terms of a ratio of the characteristic mixing to kinetic times. The mixing time is assumed equal to the inverse of the strain rate. Mellor et al. (2003) show that an activation temperature for ignition can be obtained (if a one-step global reaction is assumed) via suitable analysis of the counterflow and liquid pool ignition temperature data. Application of the ignition

model to ethane and ethene counterflow ignition data and diesel fuel liquid pool data led to correlated values of activation temperature in the range 18900 to 24300 K (23242 K for diesel fuel). The activation temperatures for ethane and ethene were found to be comparable to those presented in the literature for premixed or well-mixed fuel-oxidizer systems in similar ranges of temperature (1050 - 1350 K), pressure (1 atm), and equivalence ratio (1), confirming the validity of the approach used. No comparison of this type is possible for diesel fuel (temperatures between 1130 and 1230 K and pressure of 1 atm in this case).

Analysis of the diesel engine temperature and pressure operating range (26 to 92 bar and 893 to 1139 K) shows that it operates at conditions where there is expected to be a fundamental change in the chemistry that leads to a change in global activation temperature. Results presented in the literature for pure hydrocarbons such as n-decane, n-heptane, and α-methylnaphthalene (Ciezki and Adomeit, 1993; Pfahl et al., 1996) that are components of or are have characteristics similar to diesel fuel show that the activation temperature in the diesel operating range changes with pressure and temperature and can approach zero and in some cases become negative. Recall from Section 10.1 that Plee and Ahmad (1983) and Heywood (1988) conclude that the low activation temperatures found using the Wolfer (1938) model are due to mixing not being explicitly included in the model. However, the fact that diesel engines operate in a region where the activation temperature is not constant may also be responsible for these low activation temperatures.

Development of an appropriate mixing time for diesel sprays is the focus of the present work. Mixing time expressions under consideration are expressed in terms of the nozzle diameter and spray characteristics such as injection velocity, plume penetration, etc. The CVB and DI diesel ignition tests are being used for this work.

11.0 Combustion Model Development

11.1 Background

A phenomenological combustion model for use with quiescent chamber DI diesel engines was developed by Dr. Peter Schihl of the U. S. Army Tank and Automotive Command (TACOM) (Schihl et al., 1996; Schihl et al., 1999; Schihl, 1998). The model was subsequently modified to include the effects of swirl on the combustion event (Schihl et al., 2002). The combustion model is included in a thermodynamic cycle simulation code that allows the burn rate and cylinder pressure during the closed valve portion of the cycle to be predicted. From these predictions the engine's performance and power density may be evaluated.

Development of the phenomenological combustion model began prior to 1996. Since that time the works of Dec (1997), Flynn et al. (1999), and Higgins et al. (2000) have provided a conceptual model of the DI diesel combustion process that differs from that previously accepted in the diesel community. The Schihl combustion model is based upon the old understanding of the DI diesel combustion process.

A full description of the injection, ignition, combustion, and emissions processes is not included here for the sake of brevity. However, a brief review of these processes is warranted prior to the model derivation. Figure 3 contains a schematic of a fully developed combusting fuel plume based on the work of Dec (1997) and Flynn et al. (1999). In Fig. 3 the fuel is injected and begins to mix with the hot cylinder charge and vaporize. The vaporized fuel and charge eventually reach a standing premixed flame. The premixed flame reactants have an average equivalence ratio of ~4 and a temperature of ~825 K. The hot products of the rich premixed

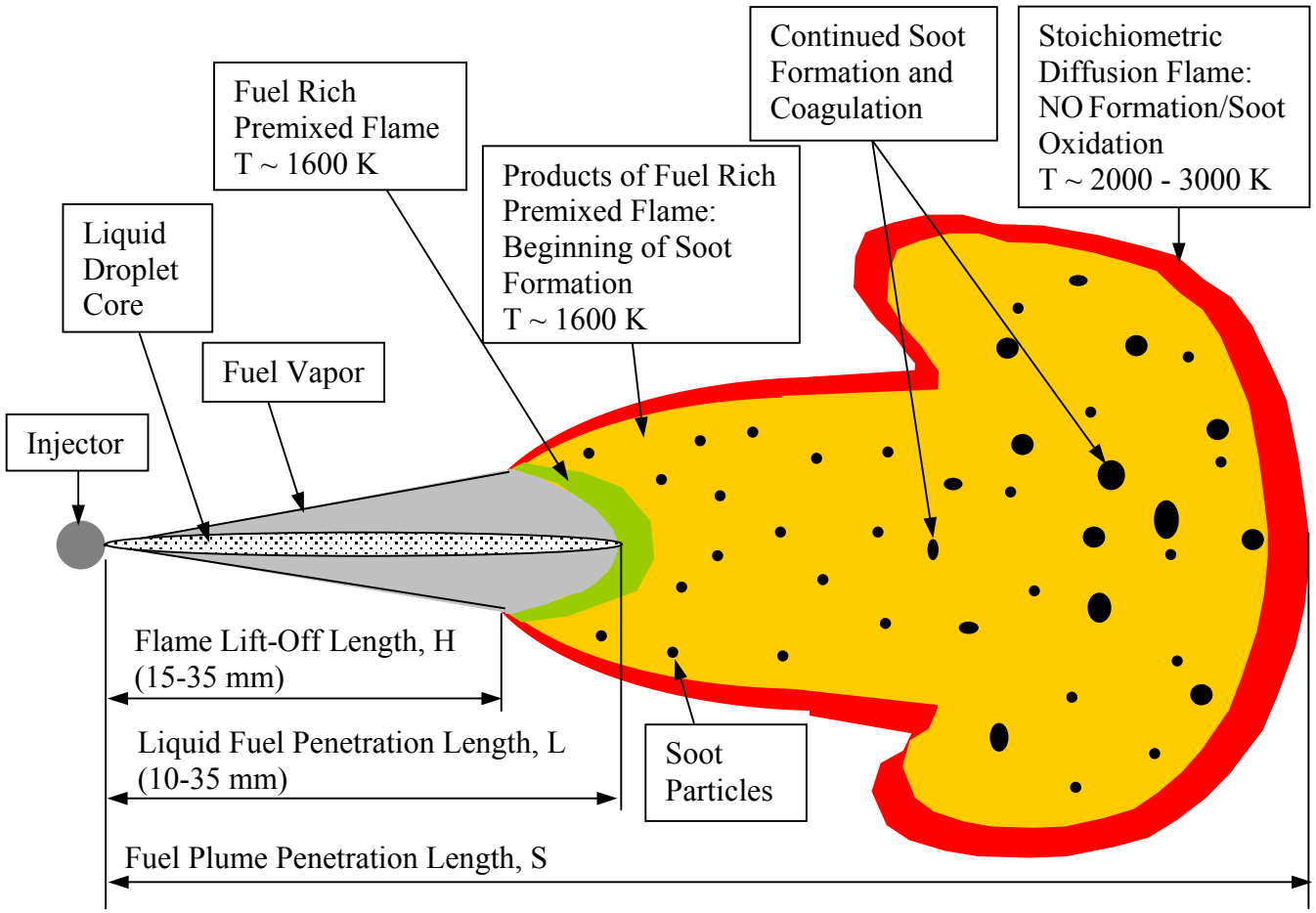

Figure 3: Schematic of a fully developed combusting fuel plume based on work of Dec (1997) and Flynn et al. (1999). Typical values of important lengths and temperatures achieved during diesel combustion have been included.

flame have a temperature of around 1600 K. The high temperature and unburned fuel in these products lead to soot formation. The rich premixed flame products continue to penetrate into the combustion chamber and entrain charge from outside the plume. At some region around the periphery of the plume exists a thin layer where the fuel and charge are at an equivalence ratio close to one. NO forms and soot oxidizes in this region where temperatures are in the range 2100 - 3000 K.

11.2 Statement of the Problem Studied

The Schihl thermodynamic cycle simulation code that includes the phenomenological combustion model was provided for use in this program (Schihl, 2001). The code is written in Fortran 77 and because of its long development history was not coded extremely efficiently. Therefore, in order to make the code more efficient and readable and because the other numerical models used at Vanderbilt are coded in C++, the first objective is to reprogram the model in C++.

Another objective of this work is to modify the combustion model to make it better conform to the conceptual model of DI diesel combustion provided by Dec (1997), Flynn et al. (1999), and Higgins et al. (2000). A secondary objective of this portion of the work is to remove some of the empirical constants found in the code by basing the model more closely on the physical and chemical processes.

Schihl and coworkers (Schihl et al., 1996; Schihl et al., 1999; Schihl, 1998; Schihl et al., 2002) validated the model using data from three engines. However, none of the data from these engines contained parametric variations in the engine control parameters. Therefore, another objective of this work is to use the parametric study done using the 0.75 L single-cylinder engine to carefully study the effects of these operating parameters on the combustion process and to ensure that the model accounts for them properly. Further, Schihl and coworkers did not have data for changes in piston bowl geometry for a given engine. The limited data with bowl geometry changes acquired using the 0.75 L single-cylinder engine are to be used to study the effect of piston bowl geometry.

11.3 Model Description

A large-scale mixing model is at the heart of the combustion model. Schihl (1998) envisions a large eddy of radius R_e and angular momentum Ω_e located in the bowl of the piston as shown in Fig. 4. Eddy angular momentum is produced (P) due to fuel injection, squish charge flow, and swirl charge flow as shown by*

$$\frac{d\Omega_e}{dt} = \frac{d}{dt}\left(0.5 m_e \omega R_e^2\right) = \dot{P}_{inj} + \dot{P}_{sq} + \dot{P}_{sw} - \dot{D}_e \qquad (7)$$

The eddy momentum is also dissipated (D) by wall friction and decay into turbulence. The production terms are modeled using characteristic velocities for each flow and characteristic length scales. Given the eddy angular momentum at IVC (determined from an analysis of the intake flow), Eq. (7) can be solved for the angular velocity (ω), which is the global mixing rate or the inverse of the characteristic time for mixing, throughout the compression and expansion strokes.

* As noted, Schihl (1998) did not include the effects of swirl in Eq. (7). Schihl (2001) included the swirl term in Eq. (7) to model combustion in engines with swirl.

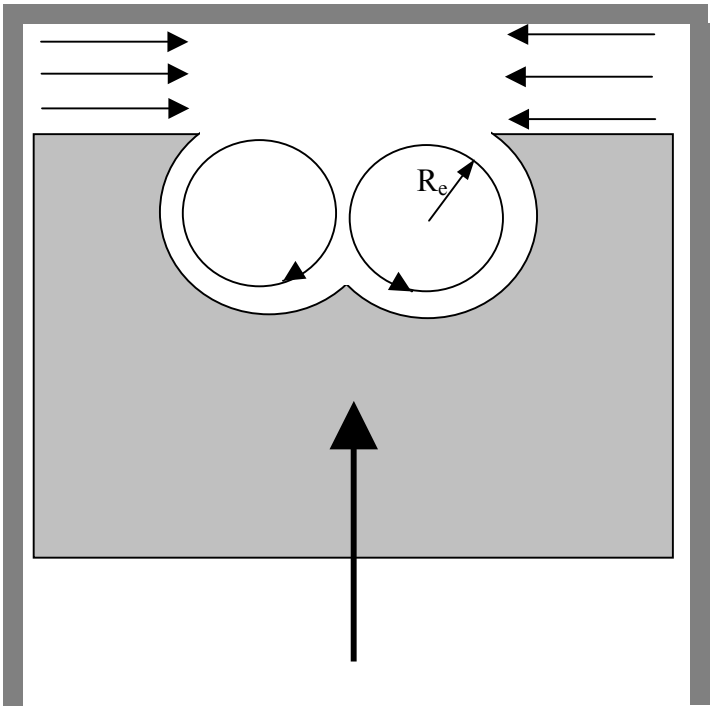

Figure 4: Schematic of a bowl-in-piston combustion chamber showing squish flow and the large-scale eddy envisioned by Schihl (1998).

Upon SOI the spray plume dispersion angle and spray plume penetration are calculated by the code using the model of Naber and Siebers (1996). Following the assumptions made in the Naber and Siebers (1996) model, the spray plume is assumed to have a conical shape as shown in Fig. 5a. In reality the plume will be deformed due to the shearing stresses exerted along the periphery of the plume and will assume the mushroom shape typical of gas phase jets, shown in Fig. 3. Ignition is assumed to occur at the tip of the spray plume following Schihl (1998) (assumption also used in ignition model of Section 10.3). This assumption is supported by the experimental works of Dec (1997) and Higgins et al. (2000).

Following Schihl (1998) the fuel burn rate (mass of fuel consumed per unit time) may be separated into the premixed burn (pb) rate and the diffusion burn (db) rate as shown by

$$\frac{dm_{f,b}}{dt} = \frac{dm_{f,pb}}{dt} + \frac{dm_{f,db}}{dt} \tag{8}$$

Schihl (1998) assumes that the premixed burn occurs only in a thin shear layer along the sides of the spray plume. However, the results of Dec (1997), Flynn et al. (1999), and Higgins et al. (2000) suggest that premixed combustion occurs throughout the volume of the spray plume head. Therefore, as an engineering approximation, upon ignition a premixed flame, encompassing the entire radial cross-section of the plume, is assumed to propagate from the tip of the spray back toward the injector as shown in Fig. 5.

Siebers and Higgins (2001) show that at the periphery of the DI diesel spray plume the premixed flame will stop propagating at the lift-off height, H, as shown in Fig. 3. These authors provide data for a lift-off height parametric study in which the effects of injection velocity (U_{inj}), nozzle diameter (d_{noz}), charge temperature (T_{ch}), and charge density (ρ_{ch}) are explored. From these data a power law was developed to fit the data and is given in Eq. (9).

$$\begin{aligned} H(m) = {} & 0.016\left(\frac{T_{ch}}{1105\ K}\right)^{-3.74}\left(\frac{\rho_{ch}}{14.8\ kg/m^3}\right)^{-0.85}\left(\frac{U_{inj}}{560\ m/s}\right)\left(\frac{d_{noz}}{0.00018\ m}\right)^{0.34} \\ & + 0.000015\left(560\ m/s - U_{inj}\right)\left(\frac{T_{ch}}{1000\ K}\right)\left(\frac{\rho_{ch}}{14.8\ kg/m^3}\right)^{-0.5}\left(\frac{d_{noz}}{0.00018\ mm}\right) \end{aligned} \tag{9}$$

The tests of Siebers (1998) show that the liquid fuel penetration will reach a quasi-steady length, L, as shown in Fig 3. A scaling law for this fueling length is presented by Siebers (1999) and is incorporated into the code. The results of Siebers and Higgins (2001) show that if the lift-off length is greater than the liquid fuel length then the premixed flame will be relatively flat across the cross-section of the spray plume, but if the liquid fuel length is greater than the lift-off height then the premixed flame will reside at the lift-off height along the periphery of the spray and just downstream of the liquid fuel length along the centerline of the spray (this case is shown in Fig. 3). To simplify the problem, the premixed flame is assumed to be flat (its axial location is not a function of the spray radius) and the steady-state distance between the premixed flame and the injector, R, given by

$$R = H \ \text{ for } \ H \geq L \ \text{ and } \ R=(H+L)/2 \ \text{ for } \ L>H \tag{10}$$

The premixed flame therefore starts at the tip of the spray and propagates back to R. The flame velocity is a function of the distance from the injector, x, and is given by

$$U_{fl,x} = \left(u' + s_L + U_{sp,x}\right) \tag{11}$$

a)

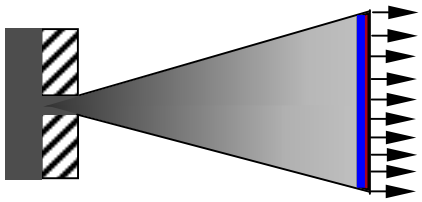

b)

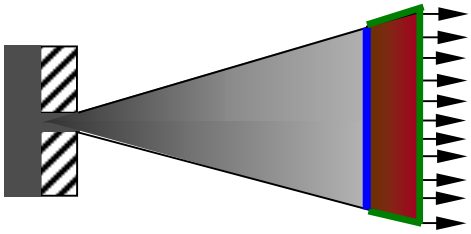

(c)

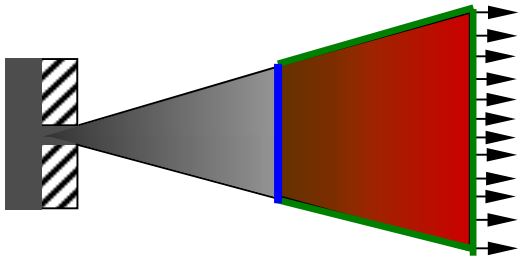

Figure 5: Schematics of the DI diesel spray plume (a) at SOC, (b) a short time after SOC, and (c) later in the combustion event when the premixed flame has reached its steady-state location. Gray is used for vapor fuel, with darker shades indicating richer mixtures. Blue lines mark the location of the premixed flame and green lines the location of the diffusion flame. Red shows the products of premixed combustion with lighter shades indicating higher temperatures.

where $U_{sp,x}$ is the velocity of the spray plume at the location of the flame calculated using the spray model of Naber and Siebers (1996), u′ is the global turbulence level calculated using an appropriate length scale and the mixing rate, ω, given by Eq. (7), and s_L is the laminar flame speed which is an input to the model.

For all cases studied thus far the conditions at the plume tip at the time of ignition are fuel rich. This result is in agreement with the experimental results of Dec (1997) and Higgins et al. (2000). Therefore, the premixed flame does not consume all of the fuel that passes through it. The mass of fuel that passes through the flame may be calculated using the spray plume model of Naber and Siebers (1996) and the known location of the flame, x. However, only the stoichiometric amount of fuel is entrained into the flame and consumed. Following Schihl (1998), the amount of fuel entrained into the flame front is given by

$$\frac{dm_{f,en}}{dt} = \left(\frac{n_f}{n_{ch}}\right)_x \tilde{\rho}_{ch} A_{fl,x} \left(u' + s_L + U_{sp,x}\right) \frac{x_{O2,ch}}{x_{O2,\phi=1}} \tag{12}$$

where $(n_f/n_{ch})_x$ is the average fuel to charge ratio at the flame location, $\tilde{\rho}_{ch}$ is the charge molar density, and A_f is the area of the flame front calculated from geometric arguments and not including the effects of flame wrinkling. The ratio of charge oxygen mole fraction, $x_{O2,ch}$, to the stoichiometric mole fraction of oxygen, $x_{O2,\phi=1}$, accounts for the fact only a portion of the fuel passing through the flame can be entrained and eventually consumed since the flame is fuel-rich and was not included by Schihl (1998). The total mass of fuel entrained into the flame can then be obtained by the integration of Eq. (12). The rate at which the fuel entrained into the premixed flame burns is given by

$$\frac{dm_{f,pb}}{dt} = \left(\frac{m_{f,en} - m_{f,pb}}{\tau_c}\right) \tag{13}$$

where the chemical time for burning is

$$\tau_c = \frac{\delta_t}{s_L} \tag{14}$$

and δ_t is the Taylor scale (Schihl, 1998).

The fuel that passes through the premixed flame unburned becomes available for diffusion combustion. The rate of diffusion burning is given by

$$\frac{dm_{f,db}}{dt} = \frac{\left(m_{f,av} - m_{f,db}\right)}{\tau_{mix}} \frac{\tau_{mix}}{\tau_{mix,util}} = \left(m_{f,av} - m_{f,db}\right) \omega \frac{\tau_{mix}}{\tau_{mix,util}} \tag{15}$$

where $m_{f,av}$ is the mass of fuel available for diffusion combustion and ω is the mixing rate (inverse of the characteristic time for mixing, τ_{mix}) given by solution of Eq. (7). The ratio $(\tau_{mix}/\tau_{mix,util})$ is a factor that adjusts the burning rate for changes in the charge composition. Schihl (1998) also included factors to account for jet expansion and flame quenching upon wall impingement.

A diagram of the spray plume just prior to the end of injection (EOI) and after the EOI is provided in Fig. 6. Once all of the fuel has passed through the premixed flame then the rich premixed flame products are surrounded by a diffusion flame that consumes most of the remaining fuel (combustion efficiencies near 100%).

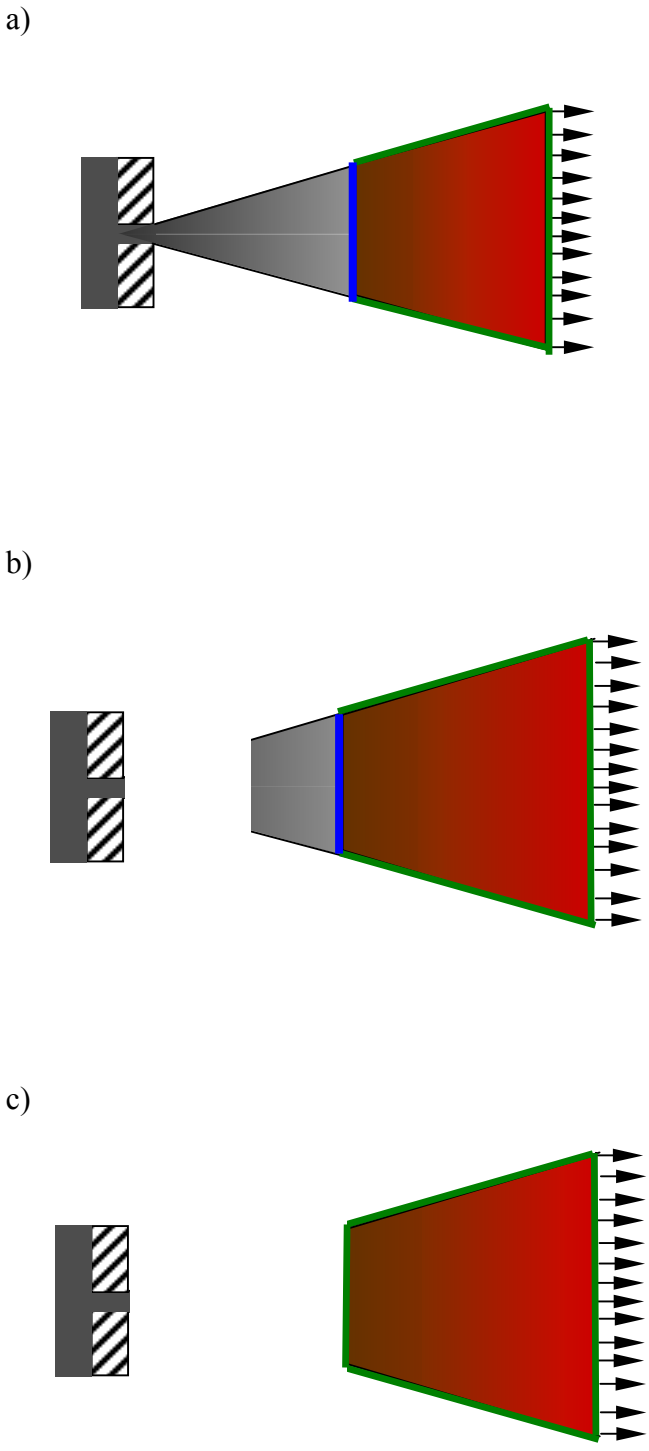

Figure 6: Schematics of the DI diesel spray plume (a) just prior to EOI, (b) a short time after EOI, and (c) after all of the fuel has passed through the premixed flame but before EOC. Gray is used for vapor fuel, with darker shades indicating richer mixtures. Blue lines mark the location of the premixed flame and green lines the location of the diffusion flame. Red shows the products of premixed combustion with lighter shades indicating higher temperatures.

11.4 Summary of the Most Important Results

The Schihl thermodynamic cycle simulation code was programmed in C++ and included in the Vanderbilt University Engine Modeling and Analysis Program (VUEMAP), a code that includes many tools for the analysis of engine data and models for the prediction of engine emissions and performance. The Schihl model is included in the code in two forms. First, it was implemented in its near original form. Second, Schihl's model was modified to more closely conform to the conceptual model of DI diesel combustion (Dec, 1997; Flynn et al., 1999; Higgins et al., 2000).

Model validation using the 0.75 L single-cylinder engine data has begun. Sample results are included in Fig. 7 and 8 for the operating conditions shown in Table 2. The graphs in Fig. 7 provide insight into how the model works. Note that a square injection rate profile has been used. In Fig. 8 the predicted apparent rate of heat release and cylinder pressure are compared to the experimental values. The results in Fig. 8 show that the predicted premixed burn rises much more rapidly than that measured experimentally, but that the peak heat release rate is matched well. The model also predicts a diffusion burn that is much faster than that found experimentally early and then reverses trend at around 10.5 CAD ATDC.

Table 2: 0.75 L single-cylinder DI diesel engine operating conditions for which sample results are shown in Fig. 7 and 8.

Engine Speed	750 RPM
Fuel Injection Pressure	100 MPa
Fuel injection quantity	0.030 g/inj.
EGR	0 %
Intake Manifold Pressure	120 kPa
Intake Manifold Temperature	353 K
Exhaust Manifold Pressure	125 kPa
Injection Timing	4.7 CAD ATDC

In Fig. 9 the experimental closed valve indicated mean effective pressure ($IMEP_{cv}$) is compared with that predicted using the model. The closed valve IMEP is used because the model predicts the cylinder pressure only for the closed valve period. The closed valve IMEP is obtained by integrating ($P_{cyl}*dV_{cyl}$) from IVC to EVO. The model is found to overpredict the $IMEP_{cv}$ for nearly all cases with the overprediction becoming greater at higher values of $IMEP_{cv}$. The predicted values are found to be fit well by a straight line.

Further refinement of the model is needed in order to improve its predictive capability. Analysis of the model and engine data is still in its preliminary stages.

12.0 NO_x Model Development

12.1 Background

The dynamic NO_x model of Psota and Mellor (2001), presented in Section 7.0, has been implemented into the cycle simulation code. In the work presented in Psota and Mellor (2001) and in Section 7.0 the required model inputs, burn rate, cylinder charge pressure, and bulk charge temperature, are derived from experimentally measured cylinder pressure. When the model is

a)

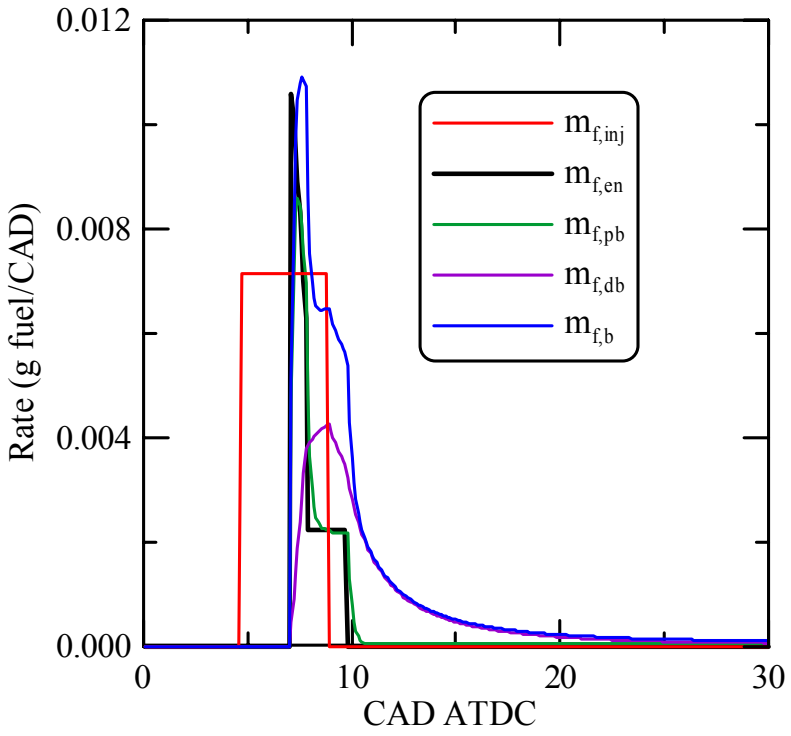

b)

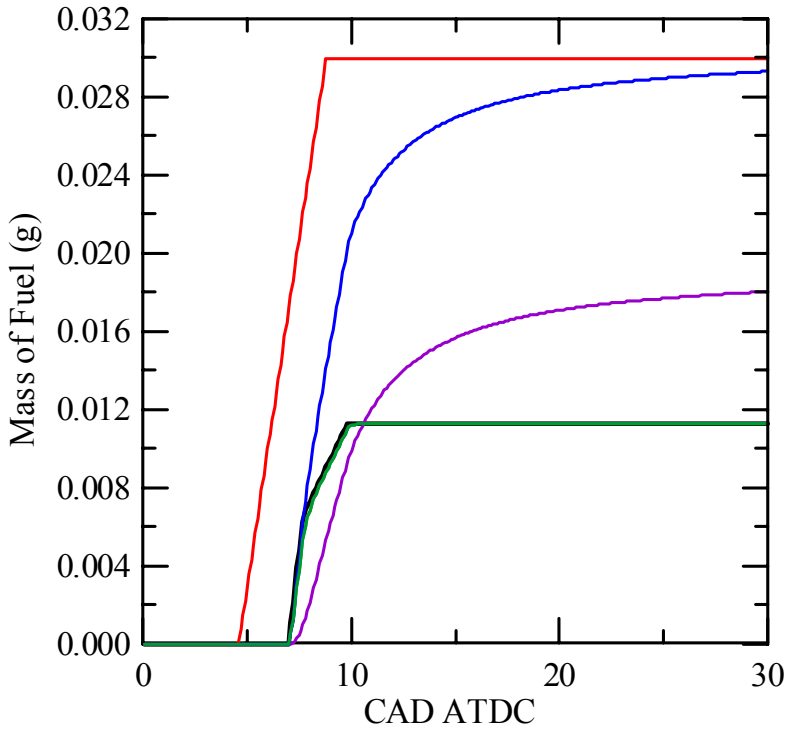

Figure 7: The rates (a) and masses (b) of fuel injected ($m_{f,inj}$), fuel entrained in the premixed flame ($m_{f,en}$), fuel consumed in by the premixed flame ($m_{f,pb}$), fuel consumed in the diffusion flame ($m_{f,db}$), and total fuel burned ($m_{f,b}$) for the operating condition shown in Table 2. The legend in (a) applies to (b) as well.

a)

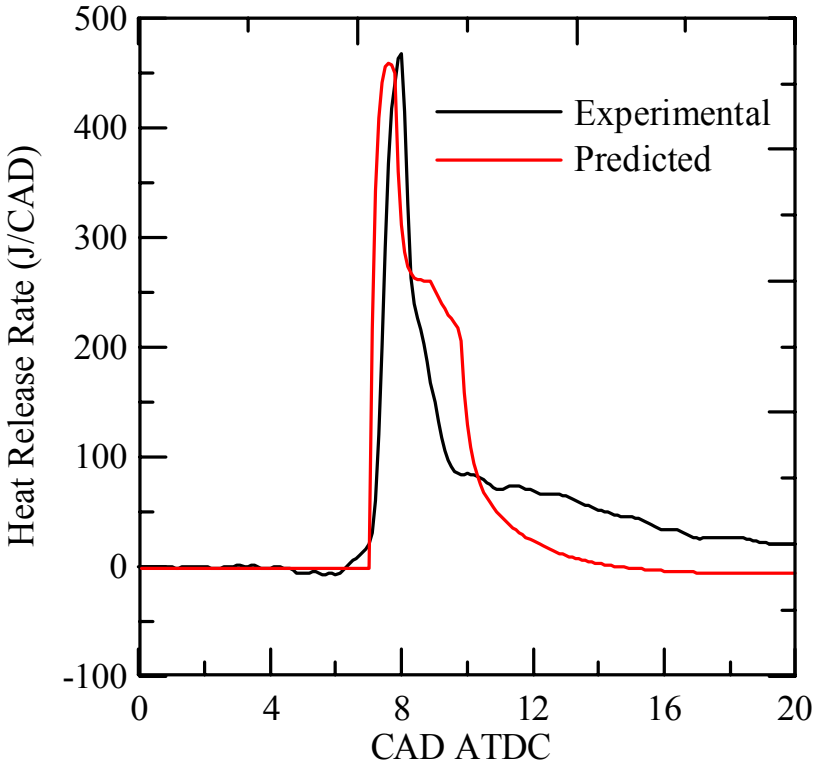

b)

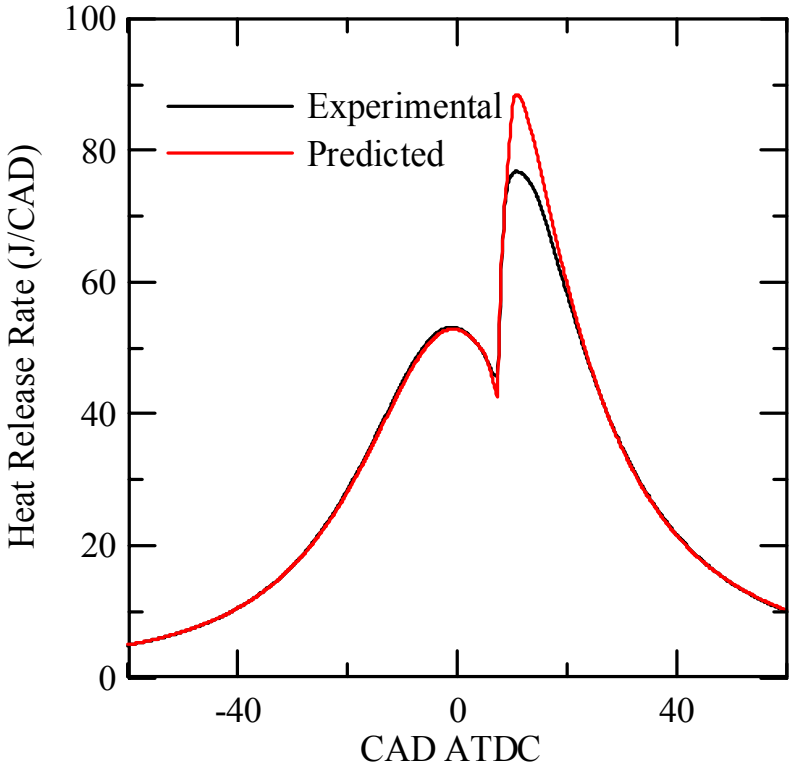

Figure 8: Comparison of the experimental and predicted (a) apparent rate of heat release and (b) cylinder pressure for the operating condition shown in Table 2.

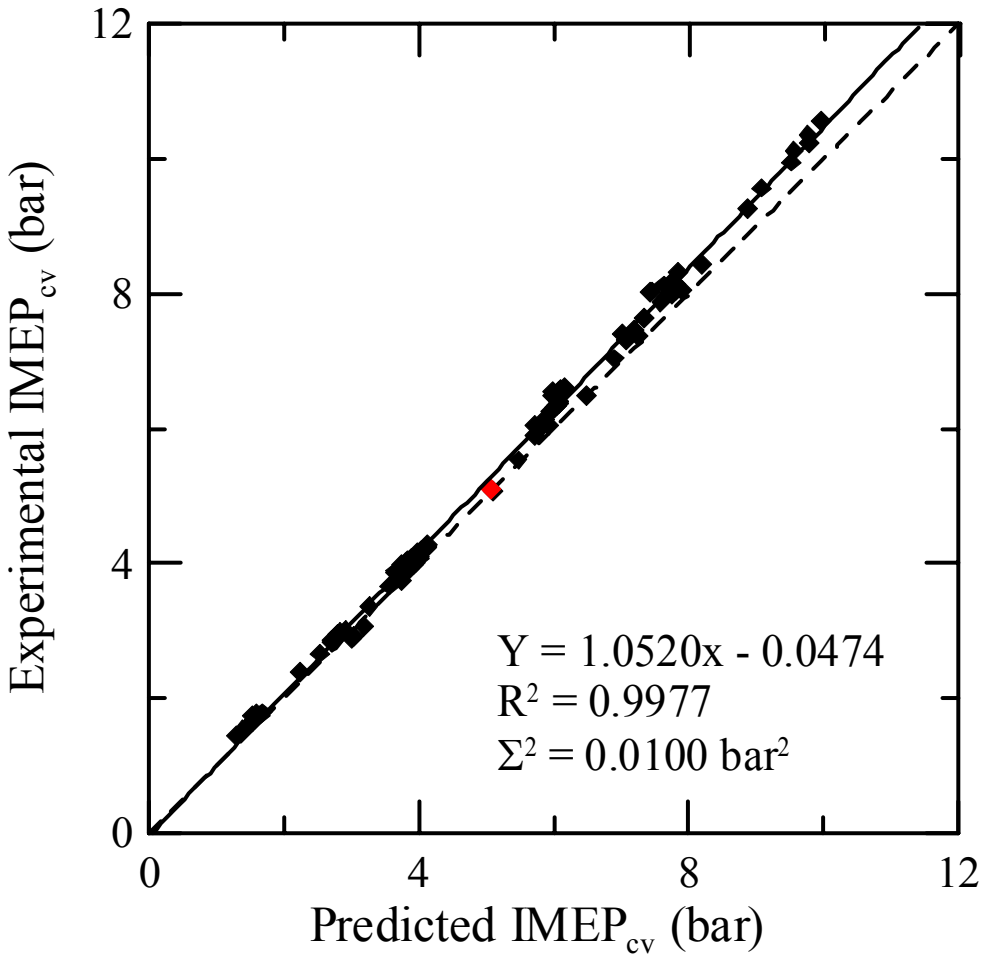

Figure 9: The closed valve indicated mean effective pressure ($IMEP_{cv}$) calculated from the experimental cylinder pressure data versus that calculated with the cycle simulation code. The dashed line has a slope of one and indicated perfect prediction. The solid line is a best-fit to the data with fit statistics given provided on the graph. The red datum is for the operating condition in Table 2.

used with the cycle simulation code these quantities are predicted and supplied to the NO_x model. Several aspects of the dynamic NO_x model are being investigated and/or modified.

12.2 Statement of the Problem Studied

The dynamic NO_x model of Psota and Mellor (2001) used the Olikara and Borman (1975) equilibrium solver to calculate the conditions in each zone of the NO_x model. This solver requires the use of proprietary equations when EGR is considered and is not valid for fuel rich mixtures. Therefore in order to extend the capabilities of the model and remove any proprietary information from the code, the equilibrium solver STANJAN (Reynolds, 1995) has replaced the Olikara and Borman (1975) solver.

Psota and Mellor (2001) define the mass in zone 1 of the model as

$$m_{1,t} = \left(\frac{dm_b}{dt} \right)_t \left(1 + \left. \frac{A}{F} \right|_{\phi=1} \right) \tag{16}$$

where (dm_b/dt) is the fuel burning rate and $A/F|_{\phi=1}$ is the stoichiometric air-fuel ratio. The subscript t indicates the parameters that are functions of time or crank position. Examination of this equation reveals that the right hand side is a mass flow rate instead of a mass. Though not explained by Psota and Mellor (2001), the zone 1 mass has been formulated in this way because the residence time of an NO forming (and possibly decomposing if using the one-zone version of the model) eddy in zone 1 is not known. Further, the mass in zone 1 should not simply be fuel and air in the case that EGR or other diluent is used, but should also contain the diluent. Therefore, Eq. (16) should read

$$m_{1,t} = \tau_{res,t} \left(\frac{dm_b}{dt} \right)_t \left(1 + \left. \frac{m_{ch}}{m_f} \right|_{\phi=1} \right) \tag{17}$$

where $\tau_{res,t}$ is the residence time of NO forming eddies passing through zone 1 at time t. Note the subscript t has been included with τ_{res} because the residence time of NO forming eddies in zone 1 can change throughout the combustion period. Inclusion of the eddy residence time in zone 1 should increase the model's ability to predict NO_x for changes in operating conditions that affect mixing. Development of an expression for $\tau_{res,t}$ using the 0.75 L single-cylinder DI diesel engine data is one of the objectives of this work.

Recall that Psota and Mellor (2001) investigated both one- and two-zone versions of the dynamic NO_x model. In the one-zone version of the NO_x model an assumption regarding the concentration of N_2O in the zone is required. Psota and Mellor (2001) assumed that N_2O is in steady-state in zone 1. Another option that is explored is to assume that reaction (R5) ($O + N_2 + M \leftrightarrow N_2O + M$) of the skeletal mechanism is in partial equilibrium. Perfectly stirred reactor simulations may also be used to determine the proper evaluation of the N_2O mechanism in zone 1.

12.3 Summary of the Most Important Results

The Olikara and Borman (1975) equilibrium solver was successfully replaced with the STANJAN (Reynolds, 1995) equilibrium solver. Discrepancies in the results obtained from the two solvers are small and can be explained by differences in the codes. The Olikara and Borman (1975) solver does not account for the effects of EGR directly, but uses a proprietary modification to the flame temperature. Further, the Olikara and Borman (1975) solver calculates

only 10 equilibrium species while the STANJAN (Reynolds, 1995) is used to calculate 20 equilibrium species.

Equation (16) was corrected with Eq. (17). To date the residence time in zone 1, $\tau_{res,t}$, has been assumed equal to one crank angle degree following the work of Psota and Mellor (2001). Replacing the $A/F|_{\phi=1}$ in Eq. (16) with $m_{ch}/m_f|_{\phi=1}$ in Eq. (17) leads to slight differences in the correlation constant, but affects the correlation statistics little. Development of an expression for the zone 1 residence time using the 0.75 L single-cylinder engine data is in its preliminary stages. The residence time is expected to be a function of injection pressure, engine speed, and other operating conditions and cylinder geometry aspects that influence mixing (Plee et al., 1981b; Duffy and Mellor, 1998). Data available to date have not been well suited for investigating this residence time because independent changes in operating conditions and injection information were not available, but data from the 0.75 L single-cylinder engine (see Section 11.0) are well suited for this work.

A comparison of the assumption that N_2O is in steady-state in the one-zone model with the assumption that reaction (R5) is in partial equilibrium was completed. The results show that the difference in the NO formation rate for either assumption is negligible.

13.0 List of All Publications and Technical Reports

(a) Papers published in peer-reviewed journals

Duffy, K. P. and Mellor, A. M. (1998), "Further developments on a characteristic time model for NO_x emissions from diesel engines," SAE Paper 982460, SAE Trans., J. Fuels and Lubricants, Vol. 107, Sect. 4, pp. 995-1012.

Mello, J. P. and Mellor, A. M. (1999), "NO_x Emissions from Direct Injection Diesel Engines with Water/Steam Dilution," SAE Paper 1999-01-0836, SAE Trans., J. Fuels and Lubricants, Vol. 108, Sect. 4, pp. 366-380.

Easley, W. L., Agarwal, A., and Lavoie, G. A. (2001), "Modeling of HCCI Combustion and Emissions Using Detailed Chemistry," SAE Paper 2001-01-1029, SAE Trans., J. Engines, Vol. 110, Sect. 3, pp. 1045-1061.

Psota, M. A. and Mellor, A. M. (2001), "Dynamic Application of a Skeletal Mechanism for DI Diesel NO_x Emissions," SAE Paper 2001-01-1984, SAE Trans., J. Fuels & Lubricants, Vol. 110, Sect. 4, pp. 1320-1334 (also listed in final report for AASERT #DAAG55-98-I-0217).

Easley, W. L., Mellor, A. M., and Gardner, T. P. (2001), "Flame Temperature Correlation of Emissions from Diesels Operated on Alternative Fuels," SAE Paper 2001-01-2014, SAE Trans., J. Fuels & Lubricants, Vol. 110, Sect. 4, pp. 1462-1481.

(b) Papers published in non-peer-reviewed journals or in conference proceedings

Easley, W. L. and Mellor, A. M. (1999), "NO Decomposition in Diesel Engines," SAE Paper 1999-01-3546.

Easley, W. L., Mellor, A. M., and Plee, S. L. (2000), “NO Formation and Decomposition Models for DI Diesel Engines,” SAE Paper 2000-01-0582.

Easley, W. L. and Mellor, A. M. (2002), "A Phenomenological Model for Autoignition in Direct Injection Diesel Engines," Proceedings of the 2002 Technical Meeting of the Central States Section of the Combustion Institute, April 7-9 (also listed in final report for AASERT #DAAG55-98-I-0217).

Yang, B., Mellor, A. M., and Chen, S. K. (2002), "Multiple Injections with EGR Effects on NO_x Emissions for DI Diesel Engines Analyzed Using an Engineering Model," SAE Paper 2002-01-2774.

(c) Papers presented at meetings, but not published in conference proceedings

None.

(d) Manuscripts submitted, but not published

Mellor, A. M., Russell, S. C., Humer, S., and Seshadri, K. (2003), "Thermal Ignition Theory Applied to Diesel Engine Autoignition," paper submitted to the Journal of Engine Research.

(e) Technical reports submitted to ARO

None.

14.0 List of All Participating Scientific Personnel Showing Any Advanced Degrees

W. L. Easley, Doctor of Philosophy in Mechanical Engineering expected in December 2003
M. A. Psota, Master of Science in Mechanical Engineering in May 2001 (also listed in final report for AASERT #DAAG55-98-I-0217)
B. Yang, Master of Science in Mechanical Engineering in May 2002

15.0 Report of Inventions

None.

Bibliography

Ahmad, T. and Plee, S. L. (1983), “Application of flame temperature correlations to emissions from a direct-injection diesel engine,” SAE Paper 831734.

Ahmad, T., Plee, S. L., and Myers, J. P. (1982), “Diffusion flame temperature – its influence on diesel particulate and hydrocarbon emissions,” presented at the International Conference on Diesel Engines for Passenger Cars and Light Duty Vehicles, Paper C101/82, Instn. Mechn. Engrs., London, October 1982.

Arnholm, C. (1997), "Mixed language programming using C++ and FORTRAN 77," http://home.online.no/~arnholm/cppf77.htm.

Aiman, W. (1973), “A critical test for models of the nitric oxide formation process in spark-ignition engines,” Fourteenth Symposium (International) on Combustion, The Combustion Institute, Pittsburgh, pp. 861-870.

Bauer, S. G. (1939), "Ignition lag in compression ignition engines," *Engineering*, Vol. 148, No. 9, P. 368-371.

Blumberg, P. and Kummer, J. T. (1971), “Prediction of NO formation in spark-ignited engines - an analysis of methods of control,” Combust. Sci. Tech., Vol. 4, pp. 73-95.

BRC (1995), "Research needed for more compact intermittent combustion propulsion systems for Army combat vehicles," Blue Ribbon Committee, Vol. I, Executive Summary and Main Body; Vol. II, Appendices, Southwest Research Institute, San Antonio, Texas.

Ciezki, H. K. and Adomeit, G. (1993), "Shock-tube investigation of self-ignition of n-heptane-air mixtures under engine relevant conditions," Combustion and Flame, Vol. 93, pp. 421-423.

Dec, J. E. (1997), “A conceptual model of DI diesel combustion based on laser-sheet imaging,” SAE Paper 970873.

Duffy, K. P. (1998), "Characteristic time model development for direct injection diesel engines," Ph.D. Dissertation, Dept. Mech. Eng., Vanderbilt University, December.

Duffy, K. P. and Mellor, A. M. (1998), "Further developments on a characteristic time model for NO_x emissions from diesel engines," SAE Paper 982460, SAE Trans., J. Fuels and Lubricants, Vol. 107, Sect. 4, pp. 995-1012.

Easley, W. L. (2000), "Nitric oxide decomposition in direct injection diesel engines," Masters Thesis, Dept. Mech. Eng., Vanderbilt University, May.

Easley, W. L. and Mellor, A. M. (1999), “NO decomposition in diesel engines,” SAE Paper 1999-01-3546.

Easley, W. L. and Mellor, A. M. (2002a), "AASERT for high power density diesel engines," Final Report for ARO Grant #DAAG55-98-I-0217, August 31.

Easley, W. L. and Mellor, A. M. (2002b), "A phenomenological model for autoignition in direct injection diesel engines," Proceedings of the 2002 Technical Meeting of the Central States Section of the Combustion Institute, April 7-9.

Easley, W. L., Mellor, A. M., and Plee, S. L. (2000), "NO formation and decomposition models for DI diesel engines," SAE Paper 2000-01-0582.

Easley, W. L., Agarwal, A., and Lavoie, G. A. (2001a), "Modeling of HCCI combustion and emissions using detailed chemistry," SAE Paper 2001-01-1029, SAE Trans., J. Engines, Vol. 110, Sect. 3, pp. 1045-1061.

Easley, W. L., Mellor, A. M., and Gardner, T. P. (2001b), "Flame temperature correlation of emissions from diesels operated on alternative fuels," SAE Paper 2001-01-2014, SAE Trans., J. Fuels & Lubricants, Vol. 110, Sect. 4, pp. 1462-1481.

Edwards, C. F., Siebers, D. L., and Hoskin, D. H. (1992), "A study of the autoignition process of a diesel spray via high speed visualization," SAE Paper 920108.

Flynn, P. F., Durrett, R. P., Hunter, G.L., zur Loye, A. O., Akinyemi, O. C., Dec, J. E., and Westbrook, C. K. (1999), "Diesel combustion: an integrated view combining laser diagnostics, chemical kinetics, and empirical validation," SAE Paper 1999-01-0509.

Foster, D. (1997), University of Wisconsin-Madison, Personal Communication.

Heywood, J. B. (1988), Internal Combustion Engine Fundamentals, McGraw-Hill, New York.

Higgins, B., Siebers, D., and Aradi, A. (2000), "Diesel-spray ignition and premixed-burn behavior," SAE Paper 2000-01-0940.

Kohketsu, S., Mori, K. and Sakai, K. (1996), "Reduction of exhaust emission with new water injection system in a Diesel engine," SAE Paper 960033.

Lavoie, G. A., Heywood, J. B., and Keck, J. C. (1970), "Experimental and theoretical study of nitric oxide formation in internal combustion engines," Combustion Science and Technology, Vol. 1, pp. 313-326.

Malte, P. C. and Pratt, D. T. (1974), "The role of energy-releasing kinetics in NO_x formation: fuel lean, jet-stirred CO-air combustion," Comb. Sci. and Tech., Vol. 9, pp. 221-231.

Mello, J. P. (1998), "Characteristic time modeling of NO_x emissions from combustion turbines and direct injection diesel engines," Masters Thesis, Dept. Mech. Eng., Vanderbilt University, May.

Mello, J. P. and Mellor, A. M. (1999), "NO_x emissions from direct injection diesel engines with water/steam dilution," SAE Paper 1999-01-0836, SAE Trans., J. Fuels and Lubricants, Vol. 108, Sect. 4, pp. 366-380.

Mellor, A. M., Mello, J. P., Duffy, K. P., Easley, W. L., and Faulkner, J. C. (1998a), "Skeletal mechanism for NO_x chemistry in diesel engines," SAE Paper 981450, 1998 SAE Transactions, Vol. 107, Sect. 4, J. Fuels and Lubricants, pp. 786-801.

Mellor, A. M., Easley, W. L., Mello, J. P., and Psota, M. A. (1998b), "DI diesel performance and emissions model," Final Report to U. S. Army Research Office for grant #DAAH04-94-G-0236, March 31.

Mellor, A. M., Russell, S. C., Humer, S., and Seshadri, K. (2003), "Thermal ignition theory applied to diesel engine autoignition," paper submitted to the Journal of Engine Research.

Naber, J. D. and Siebers, D. L. (1996), "Effects of gas density and vaporization on penetration and dispersion of diesel sprays," SAE Paper 960034.

Najt, P. M. and Foster, D. E. (1983), "Compression-ignited homogeneous charge combustion," SAE Paper 830264.

Noguchi, M., Tanaka, Y., Tanaka, T., and Takeuchi, Y. (1979), "A study on gasoline engine combustion by observation of intermediate reactive products during combustion," SAE Paper 790840.

Olikara, C. and Borman, G. L. (1975), "A computer program for calculating properties of equilibrium combustion products with some applications to IC engines," SAE Paper 750468.

Onishi, S., Jo, S. H., Shoda, K., Jo, P. D., and Kato, S. (1979), "Active thermo-atomosphere combustion (ATAC) – a new combustion process for internal combustion engines," SAE Paper 790501.

Payer, W. (2002), "Chemical-kinetic characterization of autoignition and combustion of liquid fuels," presentation dated 24 May.

Pfahl, U., Fieweger, K., and Adomeit, G. (1996), "Self-ignition of diesel-relevant hydrocarbon-air mixtures under engine conditions," Twenty-sixth Symposium (International) on Combustion, The Combustion Institute, Pittsburgh, pp. 781-789.

Plee, S. L. and Ahmad, T. (1983), "Relative roles of premixed and diffusion burning in diesel combustion," SAE Paper 831733.

Plee, S. L., Ahmad, T., and Myers, J. P. (1981a), "Flame temperature correlation for the effects of exhaust gas recirculation on diesel particulate and NO_x emissions," SAE Paper 811195.

Plee, S. L., Ahmad, T., Myers, J. P., and Siegla, D. C. (1981b), "Effects of flame temperature and air-fuel mixing on emission of particulate carbon from a divided-chamber diesel engine," Particulate Carbon - Formation During Combustion, Siegla and Smith (eds.), pp. 423-487, Plenum Press, New York.

Plee, S. L., Ahmad, T., and Myers, J. P. (1982), "Diesel NO_x emissions – a simple correlation technique for intake air effects," Nineteenth Symposium (International) on Combustion, The Combustion Institute, Pittsburgh, pp. 1495-1502.

Psota, M. A. (2001), "Dynamic application of a skeletal mechanism for DI diesel NO_x emissions," Masters Thesis, Dept. Mech. Eng., Vanderbilt University, May.

Psota, M. A. and Mellor, A. M. (2001), "Dynamic application of a skeletal mechanism for DI diesel NO_x emissions," SAE Paper 2001-01-1984, SAE Trans., J. Fuels & Lubricants, Vol. 110, Sect. 4, pp. 1320-1334.

Reynolds, W. C. (1995), "STANJAN Version 3.93," Dept. Mech. Eng., Stanford University.

Sato, J., Konishi, K., Okada, H., and Niioka, T. (1986), "Ignition process of fuel spray injected into high pressure high temperature atmosphere," 21st Symposium (International) on Combustion, The Combustion Institute, pp. 695-702.

Schihl, P. J. (1998), "Development of global mixing, combustion, and ignition models for quiescent chamber direct-injection diesel engines," Ph.D. Dissertation, Dept. Mech. Eng., University of Michigan, Ann Arbor, MI.

Schihl, P. J. (2001), Personal communication to William Easley, January 2, attached Large Scale Combustion Model Code.

Schihl, P., Bryzik, W., and Atreya, A. (1996), "A large scale mixing model for a quiescent chamber direct injection diesel," SAE Paper 961040.

Schihl, P. J., Atreya, A., Bryzik, W., and Schwarz, E. (1999), "Simulation of combustion in direct-injection low swirl heavy-duty type diesel engines," SAE Paper 1999-01-0228.

Schihl, P., Tasdemir, J., Schwarz, E. and Bryzik, W. (2002), "Development of a zero-dimensional heat release model for application to small bore diesel engines," SAE Paper 2002-01-0073.

Seshadri, K. (2002), "Chemical kinetic characterization of autoignition and combustion of diesel and JP-8," ARO/AFOSR Contractors Meeting in Chemical Propulsion, Dayton, OH.

Siebers, D. L. (1998), "Liquid-phase fuel penetration in diesel sprays," SAE Paper 980809.

Siebers, D. L. (1999), "Scaling liquid-phase fuel penetration in diesel sprays based on mixing-limited vaporization," SAE Paper 1999-01-0528.

Siebers, D. L. (2002), Personal communication to W. L. Easley, October.

Siebers, D. and Higgins, B. (2001), "Flame lift-off on direct-injection diesel sprays under quiescent conditions," SAE Paper 2001-01-0530.

Voiculescu, I. A. and Borman, G. L. (1978), “An experimental study of diesel engine cylinder-averaged NO_x histories,” SAE Paper 780228.

Wolfer, H. H. (1938), "Ignition lag in diesel engines," VDI-Forschungsheft No. 392, Translated by Royal Aircraft Establishment, Farnborough Library No. 358, U.D.C. No. 621-436.047, Aug. 1959.

Yang, B. (2002), "Effects of advanced injection strategies on direct injection diesel emissions," Masters Thesis, Dept. Mech. Eng., Vanderbilt University, May.

Yang, B., Mellor, A. M., and Chen, S. K. (2002), "Multiple injections with EGR effects on NO_x emissions for DI diesel engines analyzed using an engineering model," SAE Paper 2002-01-2774.